IMA Journal of Numerical Analysis (2005) Page 1 of 21
doi: 10.1093/imanum/dri000

Pointwise error estimates for a singularly perturbed time-dependent semilinear reaction-diffusion problem*

NATALIA KOPTEVA AND SIMONA BLANCA SAVESCU†

Mathematics and Statistics Department, University of Limerick, Limerick, Ireland.

An initial-boundary-value problem for a semilinear reaction-diffusion equation is considered. Its diffusion parameter ε^2 is arbitrarily small, which induces initial and boundary layers. It is shown that the conventional implicit method might produce incorrect computed solutions on uniform meshes. Therefore we propose a stabilized method that yields a unique qualitatively correct solution on any mesh. Constructing discrete upper and lower solutions, we prove existence and investigate the accuracy of discrete solutions on layer-adapted meshes of Bakhvalov and Shishkin types. It is established that the two considered methods enjoy second-order convergence in space and first-order convergence in time (with, in the case of the Shishkin mesh, a logarithmic factor) in the maximum norm, if $\varepsilon \leqslant C(N^{-1}+M^{-1/2})$, where N and M are the numbers of mesh intervals in the space and time directions, respectively. Numerical results are presented that support the theoretical conclusions.

Keywords: semilinear reaction-diffusion, singular perturbation, maximum norm error estimate, Bakhvalov mesh, Shishkin mesh, upper and lower solutions.

1. Introduction

Consider the singularly perturbed semilinear reaction-diffusion equation

$$\mathcal{T}u \equiv \varepsilon^2[u_t - u_{xx}] + f(x,t,u) = 0 \qquad \text{for } (x,t) \in (0,1)\times(0,T], \tag{1.1a}$$

subject to the boundary and initial conditions

$$u(0,t) = g_0(t), \quad u(1,t) = g_1(t), \qquad t \in [0,T], \tag{1.1b}$$

$$u(x,0) = \varphi(x), \qquad x \in [0,1]. \tag{1.1c}$$

Here ε is a small positive parameter, and the functions f, g_0, g_1 and φ are sufficiently smooth; furthermore, at the corners $(0,0)$ and $(1,0)$ of our domain we assume the standard compatibility conditions $g_0(0) = \varphi(0)$ and $g_1(0) = \varphi(1)$. Equations of type (1.1a), with a small parameter multiplying the operator $\frac{\partial}{\partial t} - \frac{\partial^2}{\partial x^2}$ (or $\frac{\partial}{\partial t} - \triangle$ in more dimensions), frequently arise in modelling fast chemical reactions and other applications; see, e.g., Winfree & Jahnke (1989); Fife & Gill (1991); Soane *et al.* (2005).

It is often assumed in the numerical analysis literature that $f_u(x,t,u) > 0$ for all $(x,t,u) \in [0,1]\times[0,T]\times\mathbb{R}$. This global condition is nevertheless rather restrictive as mathematical models of chemical and biological processes typically involve reaction terms, such as $f(x,t,u)$ in (1.1a), that are *non-monotone* with respect to the solution. Hence we drop the assumption that $f_u > 0$ and consider problem (1.1) under weaker assumptions, described in §3, that intrinsically arise from the asymptotic analysis of this problem.

*This publication has emanated from research conducted with the financial support of Science Foundation Ireland under the Research Frontiers Programme 2008; Grant 08/RFP/MTH1536.

†Email: Natalia.Kopteva@ul.ie; Simona.Savescu@ul.ie

The reduced problem of (1.1) is defined by formally setting $\varepsilon = 0$ in (1.1a), i.e.

$$f(x,t,u_0(x,t)) = 0 \qquad \text{for } (x,t) \in (0,1)\times(0,T). \tag{1.2}$$

As f_u is not necessarily positive, this equation might have multiple solutions, and any solution u_0 of (1.2) does not in general satisfy the boundary and initial conditions in (1.1b) and (1.1c). Similarly, the steady-state version of (1.1) might have multiple solutions. In contrast, the initial-boundary-value problem (1.1) always has at most one solution; see Proposition 2.1 below. Therefore, if problem (1.1) is solved numerically, it is desirable that the computed solution enjoys a similar property.

We discretize (1.1) on a tensor-product mesh $\{(x_i,t_j)\}$ in $[0,1]\times[0,T]$, where $0 = x_0 < x_1 < \cdots < x_N = 1$ and $0 = t_0 < t_1 < \cdots < t_M = T$, and we use the notation $h_i := x_i - x_{i-1}$ and $k_j = t_j - t_{j-1}$ for the local mesh sizes. One standard implicit discretization of (1.1) is given by

$$\mathcal{T}^h U_{ij} := \varepsilon^2 [\delta_t - \delta_x^2] U_{ij} + f(x_i,t_j,U_{ij}) = 0 \tag{1.3}$$

for $i = 1,\ldots,N-1$ and $j = 1,\ldots,M$, where we use backward differencing in time and the standard three-point discretization in space:

$$\delta_t U_{ij} := \frac{U_{ij} - U_{i,j-1}}{k_j}, \qquad \delta_x^2 U_{ij} := \frac{2}{h_i + h_{i+1}}\Big(\frac{U_{i+1,j} - U_{ij}}{h_{i+1}} - \frac{U_{ij} - U_{i-1,j}}{h_i}\Big).$$

We also set $U_{i,0} = \varphi(x_i)$ for $i = 0,\ldots,N$, and $U_{0,j} = g_0(t_j)$, $U_{N,j} = g_1(t_j)$ for $j = 1,\ldots,M$.

Note that the conventional method (1.3), when applied on a uniform mesh in time, might yield incorrect and unstable computed solutions; see Figure 1 (left and centre). Here problem (1.1) was solved with $f = (2-u)(u-1)u(u+1)$ and $\varphi = 0.1 + 2x(1-x)$, $g_0 = g_1 = 0.1$. We observe that $u(x,2)$, which is effectively the steady-state solution, is entirely different from the computed solutions at $t = 2$. We also refer the reader to Figure 3 (left), where the numerical method (1.3) is applied to a more complicated problem (6.1) and again yields an incorrect computed solution (which now looks stable and can be easily mistaken for a correct one; compare with Figure 2 (left)).

This instability can be explained noting that if $\varepsilon \ll 1$, in particular, if $\varepsilon^2 \ll k_j$, then the time derivative term $\varepsilon^2 \delta_t U$, being $O(\varepsilon^2/k_j)$, becomes negligible; thus at each time level we effectively solve a steady-state discrete equation and therefore at each time level we might get any of the multiple steady-state solutions. Furthermore, the space derivative term $\varepsilon^2 \delta_x^2 U$, being $O(\varepsilon^2/(h_i + h_{i+1})^2)$, might become negligible too, in which case we effectively solve the algebraic equation $f(x_i,t_j,U_{ij}) = 0$ at each mesh node, where this occurs.

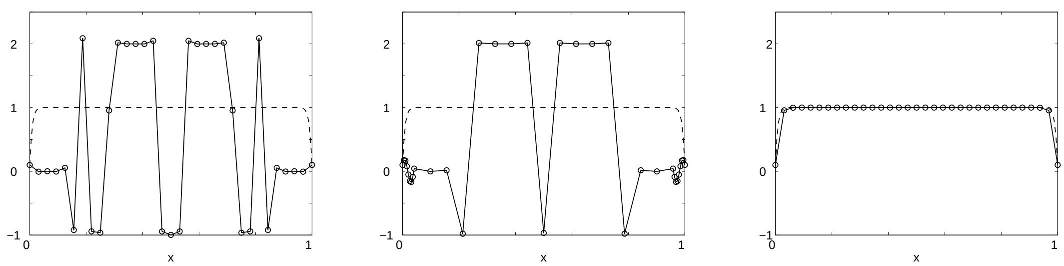

FIG. 1. Computed solutions at $t = 2$ vs. the exact solution (dashed curve) for various methods; $\varepsilon = 10^{-2}$, $N = 32$, $M = N^2$. Left and centre: conventional method (1.3) fails to yield correct computed solutions on the uniform mesh (left), and even if the Shishkin mesh (described in §5.1(b); $\gamma = 1$) is used in space combined with the uniform mesh in time (centre). Right: stabilized method (2.1) with $\hat{C} = 2$ on the uniform mesh yields a qualitatively correct computed solution.

As the conventional implicit method (1.3) might produce incorrect and unstable computed solutions, below we propose a stabilized method (2.1), which is obtained from (1.3) by artificially strengthening the time derivative term. The added stabilization is controlled by a constant parameter $\hat{C} \geqslant 0$. Since the original problem always has at most one solution (while the conventional method might lack this property), we propose that this stabilization parameter $\hat{C}$ should be chosen so that the discrete problem also has at most one solution. Under this choice of $\hat{C}$ (prescribed by Proposition 2.2), our numerical results suggest that switching to the stabilized method cures the instability and yields qualitatively-correct computed solutions on any mesh; see Figures 1 and 3.

Furthermore, we shall particularly examine solutions of (1.1) that exhibit boundary and initial layers. For such solutions, we aim to resolve the layers and thus attain high accuracy in the entire domain. Therefore we shall consider both conventional and stabilized discretizations on layer-adapted meshes of Bakhvalov and Shishkin types, and theoretically investigate their convergence in the maximum norm. Our analysis invokes the theory of lower and upper solutions.

The paper is organized as follows. In the next §2, we introduce a stabilized discretization of (1.1), establish uniqueness of continuous and discrete solutions, and therefore propose the choice of the stabilization parameter. The following §3 presents our assumptions on problem (1.1). In §4 we discuss asymptotic properties of solutions of (1.1) and construct lower and upper solutions. In §5, layer-adapted meshes for solving (1.1) are described, and discrete analogues of the upper and lower solutions are used to obtain tight upper and lower bounds on the computed solutions. Precise convergence results for the conventional method (1.3) and the stabilized method (2.1) are then derived on Bakhvalov and Shishkin meshes. In §6, numerical results illustrate the sharpness of our theoretical error estimates. Finally, §7 summarizes our conclusions.

Note that an asymptotic analysis of a version of (1.1) with Neumann boundary conditions, which we partly imitate in §4, was given in (Vasil'eva *et al.*, 1995, §3.2.3). We also refer the reader to asymptotic and numerical analyses for one- and two-dimensional steady-state versions of (1.1) by Fife (1973); Nefedov (1995); Sun & Stynes (1996); Kopteva & Stynes (2004); Kopteva (2007).

Notation. Throughout this paper we let C denote a generic positive constant that may take different values in different formulas, but is always independent of N, M and ε. A subscripted C (e.g., C_1) denotes a positive constant that is independent of N, M and ε and takes a fixed value. For any two quantities w_1 and w_2, the notation $w_1 = O(w_2)$ means $|w_1| \leqslant C w_2$.

2. Stabilized discretization. Uniqueness of continuous and discrete solutions

To stabilize the conventional method (1.3), we generalize it, for some constant $\hat{C} \geqslant 0$, as follows:

$$\hat{\mathfrak{T}}^h \hat{U}_{ij} := [\hat{\varepsilon}_j^2\, \delta_t - \varepsilon^2\, \delta_x^2]\, \hat{U}_{ij} + f(x_i, t_j, \hat{U}_{ij}) = 0, \qquad \hat{\varepsilon}_j^2 = \max\{\varepsilon^2, \hat{C} k_j\}. \tag{2.1}$$

Here, as usual, we set $\hat{U}_{i,0} = \varphi(x_i)$ for $i = 0, \ldots, N$, and $\hat{U}_{0,j} = g_0(t_j)$, $\hat{U}_{N,j} = g_1(t_j)$ for $j = 1, \ldots, M$. Clearly, (1.3) is a particular case of (2.1) with $\hat{C} = 0$. Compared to (1.3), in (2.1) we artificially strengthen the time derivative term, replacing $\varepsilon^2 \delta_t$ by $\hat{\varepsilon}^2 \delta_t$, which does not influence the consistency order of the method, but under an appropriate choice of $\hat{C}$, always yields at most one discrete solution; see Proposition 2.2 below. Furthermore, Figures 1 and 3 illustrate that the instability that we have observed, is indeed cured by switching to the stabilized method (2.1) in which $\hat{C}$ is chosen using Proposition 2.2.

For uniqueness of solutions of the continuous problem (1.1) and discrete problems (1.3) and (2.1) we have the following results.

PROPOSITION 2.1 (UNIQUE CONTINUOUS SOLUTION) Problem (1.1) has at most one solution.

Proof. The proof imitates the argument in (Pao, 1992, Theorem 5.1) and we sketch it here for completeness. Suppose (1.1) has two solutions u and $\bar{u}$ on $[0,1]\times[0,T]$. Then $|u|,|\bar{u}|\leqslant K_1$ and therefore $f_u \geqslant -K_2$ in $[0,1]\times[0,T]\times[-K_1,K_1]$ for some positive constants K_1 and K_2, which may depend on ε and T. Using the standard linearization technique and then the transformation $z := (\bar{u}-u)e^{-tK_2/\varepsilon^2}$, we get $\varepsilon^2[\frac{\partial}{\partial t}-\frac{\partial^2}{\partial x^2}]z+(K_2+p)z=0$ where $p=p(x,t)=\int_0^1 f_u(x,t,u+s[\bar{u}-u])\mathrm{d}s \geqslant -K_2$. Since z vanishes for $x=0,1$ and for $t=0$, by the maximum principle (Protter & Weinberger, 1999, Chapter 3), we have $z=0$ for all (x,t). Note that this argument relies on f_u being continuous for all $u\in\mathbb{R}$ (otherwise, we refer the reader to a solution non-uniqueness example in (Pao, 1992, §1.6)). □

PROPOSITION 2.2 (UNIQUE COMPUTED SOLUTION) Let $\hat{U}_{ij}$ be a solution of (2.1) and let $\hat{\varepsilon}_j^2 > C^* k_j$ for some $C^*\geqslant 0$. If $f_u \geqslant -C^*$ for all x,t,u, then $\hat{U}$ is a unique solution of (2.1). If $K_1 \leqslant \hat{U}_{ij} \leqslant K_2$ for some constants K_1 and K_2, and $f_u\geqslant -C^*$ in $[0,1]\times[0,T]\times[K_1,K_2]$, then $\hat{U}$ is a unique solution of (2.1) between K_1 and K_2.

Proof. We imitate the proof of (Pao, 1985, Theorem 3.1), where the non-singularly-perturbed case of $\varepsilon=\hat{\varepsilon}_j=1$ was considered. Compared to the cited result by Pao, our proposition reveals the role of the small parameter $\hat{\varepsilon}_j$ in the uniqueness condition $\hat{\varepsilon}_j^2 > C^* k_j$.

Let $\bar{U}_{ij}$ be another solution of (2.1) and introduce $Z_{ij} := (\bar{U}_{ij}-\hat{U}_{ij})\prod_{l=1}^{j}(1+k_l\,\mu_l/\hat{\varepsilon}_l^2)^{-1}$. A calculation shows that $\hat{\varepsilon}_j^2\delta_t Z_{ij}+\mu_j Z_{ij} = (\hat{\varepsilon}_j^2+k_j\,\mu_j)[\delta_t(\bar{U}_{ij}-\hat{U}_{ij})]\prod_{l=1}^{j}(1+k_l\,\mu_l/\hat{\varepsilon}_l^2)^{-1}$. Therefore, applying the standard linearization, we arrive at

$$\frac{\hat{\varepsilon}_j^2}{1+k_j\,\mu_j/\hat{\varepsilon}_j^2}\delta_t Z_{ij}-\varepsilon^2\delta_x^2 Z_{ij}+\Big(\frac{\mu_j}{1+k_j\,\mu_j/\hat{\varepsilon}_j^2}+p_{ij}\Big)Z_{ij}=0,$$

where $p_{ij} := \int_0^1 f_u(x_i,t_j,\hat{U}_{ij}+s[\bar{U}_{ij}-\hat{U}_{ij}])\mathrm{d}s \geqslant -C^*$. As for some constant $\tilde{C}^* > C^*$ we have $\hat{\varepsilon}_j^2 \geqslant \tilde{C}^* k_j$, then $\mu_j/(1+\mu_j k_j\hat{\varepsilon}_j^{-2}) \geqslant \mu_j/(1+\mu_j/\tilde{C}^*)$ and choosing μ_j sufficiently large, we can always make $\mu_j/(1+\mu_j/\tilde{C}^*)$ sufficiently close to $\tilde{C}^*$, and therefore, exceeding C^*. Now, for the coefficient at Z_{ij} we have $\mu_j/(1+\mu_j k_j\hat{\varepsilon}_j^{-2})+p_{ij}\geqslant 0$. So, recalling that $Z_{ij}=0$ for $x_i=0,1$ and $t_j=0$, by the discrete maximum principle, we get $Z_{ij}=0$ for all i, j. □

REMARK 2.3 To apply Proposition 2.2 to the conventional method (1.3), we have to impose a very restrictive *global* condition $k_j < \varepsilon^2/C^*$ on the time step k_j, which would result in a very inefficient method (as it typically suffices to refine the mesh only where the solution changes very rapidly). In contrast, choosing $\hat{C}$ sufficiently large in (2.1) so that $\hat{C} > C^*$, where C^* is from Proposition 2.2, we can always ensure that there is at most one computed solution.

REMARK 2.4 Furthermore, it can be shown theoretically that if $k_j \gg \varepsilon^2$ for any j, then the conventional discrete problem (1.3) might have multiple computed solutions both when the mesh in space is uniform or of Bakhvalov/Shishkin type (as described in §5.1). The proof relies on the discrete steady-state problem having multiple solutions (as $\varepsilon^2\delta_t U_{ij}$ is sufficiently small, certain lower and upper solutions of the discrete steady-state problem also work as lower and upper solutions of (1.3) at time level j).

REMARK 2.5 At this stage, the reader might get confused by what we mean by multiplicity of computed solutions, as running a computer code we get (at most) one computed solution (not many!). Indeed, applying a particular iterative method (e.g., Newton's method) with a particular initial guess, we get one solution of our discrete nonlinear problem, so no multiplicity might be observed in the numerical experiments. However, if the discrete nonlinear problem has multiple solutions, applying a different iterative method, or even simply modifying an initial guess, we might get another solution of this discrete problem (see also Figure 4). The danger of the situation when a continuous problem has a unique solution, while its discretization has many, lies in the observation that running a computer code one might get a completely incorrect computed solution, as illustrated by Figures 1 and 3.

3. Assumptions on the continuous problem

We shall examine solutions of (1.1) that exhibit boundary and initial layers. (In general, solutions of (1.1) may also have interior transition layers, which we will consider in a future paper.) As was announced in the introduction, we drop the restrictive global assumption that $f_u(x,t,u) > 0$ for all $(x,u) \in [0,1]\times[0,T]\times\mathbb{R}^1$, and consider problem (1.1) under the following weaker assumptions.

- It has a *stable reduced solution*, i.e. there exists a sufficiently smooth solution u_0 of (1.2) such that
$$f_u(x,t,u_0(x,t)) > \gamma^2 > 0 \quad \text{for all } (x,t)\in[0,1]\times[0,T]. \tag{A1}$$
- The boundary conditions satisfy
$$\int_{u_0(l,t)}^{v} f(l,t,s)\,\mathrm{d}s > 0 \qquad \text{for all } v\in\big(u_0(l,t),g_l(t)\big]', \qquad l=0,1, \quad t\in[0,T]. \tag{A2}$$
Here the notation $(a,b]'$ is defined to be $(a,b]$ when $a<b$ and $[b,a)$ when $a>b$, while $(a,b]'=\emptyset$ when $a=b$.
- The initial condition is in the *domain of attraction* of the reduced solution u_0, i.e. it satisfies
$$s\,f(x,0,u_0(x,0)+s) > 0 \qquad \text{for all } s\in(0,\varphi(x)-u_0(x,0)]', \qquad x\in[0,1]. \tag{A3}$$

Note that if $g_l(t)\approx u_0(l,t)$ for $l=0$ or $l=1$, then (A2) follows from (A1) combined with (1.2), while if $g_l(t)=u_0(l,t)$ at some point $t\in[0,T]$, then (A2) does not impose any restriction on g_l at this point. Similarly, if $\varphi(x)\approx u_0(x,0)$, then (A3) follows from (A1) combined with (1.2), while $\varphi(x)=u_0(x,0)$ does not impose any restriction on φ at this point.

The term "domain of attraction", which appears in the description of (A3), is more frequently applied to initial-value problems. E.g., for the ordinary differential equation $\varepsilon^2\tilde u_t + f(x,t,\tilde u)=0$ subject to the initial condition $\tilde u(x,0)=\varphi(x)$ (compare with (1.1)), assumption (A3) implies that $\tilde u(x,t)\approx u_0(x,t)$ for $t\gg\varepsilon^2$, i.e. away from $t=0$, the solution $\tilde u$ becomes close to the reduced solution u_0, not any other solution of the reduced problem (1.2); see (Vasil'eva *et al.*, 1995, Section 2.1).

Conditions (A1), (A2), (A3) intrinsically arise from the asymptotic analysis of problem (1.1) and guarantee that there exists a unique solution u of (1.1), which exhibits boundary layers of width $O(\varepsilon|\ln\varepsilon|)$ at $x=0,1$ and an initial layer of width $O(\varepsilon^2|\ln\varepsilon|)$ at $t=0$, while $u\approx u_0$ in the interior subdomain of $(0,1)\times(0,T]$ away from $x=0,1$ and $t=0$; see Theorem 4.9 for a precise statement. We also refer the reader to Kopteva & Stynes (2004) for a detailed discussion of (A1), (A2) in one dimension, and also to Remark 4.4 on the role of assumption (A3).

We make two further simplifying assumptions to facilitate our presentation. To avoid considering cases, assume that
$$u_0(l,t)\leqslant g_l(t) \ \text{ for } \ l=0,1, \ t\in[0,T]; \qquad u_0(x,0)\leqslant\varphi(x) \ \text{ for } \ x\in[0,1]. \tag{3.1}$$

To ensure that problem (1.1) has sufficiently smooth solutions, we also impose the *first-order compatibility* conditions $\varepsilon^2[g_l'(0) - \varphi''(l)] + f(l,0,\varphi(l)) = 0$ for $l = 0,1$, i.e. at the domain corners $(0,0)$ and $(1,0)$. Dropping the $O(\varepsilon^2)$ terms, we get $f(l,0,\varphi(l)) = 0$ for $l = 0,1$. Combining these with (A3), we conclude that

$$\varphi(l) = g_l(0) = u_0(l,0) \qquad \text{for } l = 0,1. \tag{3.2}$$

More generally, all our further results apply to problem (1.1) with $f(x,t,u) = f(x,t,u,\varepsilon)$, $g_l(t) = g_l(t,\varepsilon)$, for $l = 1,2$, and $\varphi(x) = \varphi(x,\varepsilon)$, where f, g_1, g_2 and φ are sufficiently smooth functions of ε. In this case the first-order compatibility conditions imply that $f(l,0,\varphi(l)) = O(\varepsilon^2)$ for $l = 0,1$, and therefore (3.2) will be replaced by a similar relation $\varphi(l) = g_l(0) = u_0(l,0) + O(\varepsilon^2)$.

4. Asymptotic analysis, upper and lower solutions

We start this section by presenting a standard second-order asymptotic expansion. Furthermore, we shall modify it to construct certain upper and lower solutions that provide tight control on the solutions of our problem (1.1).

We shall use the functions

$$F(x,t,s) := f(x,t,u_0(x,t)+s), \qquad \tilde{F}(x,t,s;p) := f(x,t,u_0(x,t)+s) - ps.$$

The perturbed version $\tilde{F}$ of the function F is used, with $|p|$ sufficiently small, in the construction of upper and lower solutions. In the constructions that follow, a tilde will always denote a perturbed function. The perturbed functions always depend on the parameter p, but we will sometimes not show the explicit dependence. Thus, we will sometimes write $\tilde{F}(x,t,s)$ for $\tilde{F}(x,t,s;p)$. Note that $\tilde{F}(x,t,0) = 0$ implies $\tilde{F}_x(x,t,0) = 0$, $\tilde{F}_{xx}(x,t,0) = 0$ and $\tilde{F}_t(x,t,0) = 0$, and therefore we have

$$|\tilde{F}_x(x,t,s)| \leqslant C|s|, \qquad |\tilde{F}_{xx}(x,t,s)| \leqslant C|s|, \qquad |\tilde{F}_t(x,t,s)| \leqslant C|s|. \tag{4.1}$$

We will occasionally use, for any sufficiently smooth function g, the notations

$$g\big|_a^b = g(b) - g(a), \qquad g\big|_{a;b}^c = g(c) - g(b) - g(a). \tag{4.2}$$

Since $g(a+b) - g(a) - g(b) + g(0) = ab\,g''(\theta)$ for some θ such that $|\theta| \leqslant |a| + |b|$, we see that $g(0) = 0$ implies $g\big|_{a;b}^{a+b} = O(|ab|)$. Therefore, under this notation, $\tilde{F}(x,t,0) = 0$ implies that

$$\tilde{F}(x,t,\cdot)\Big|_{a;b}^{a+b} = O(|ab|). \tag{4.3}$$

Under our assumptions (A1)-(A3), the solution of problem (1.1) exhibits boundary layers near $x = 0$ and $x = 1$, and an initial layer near $t = 0$. Since the construction of the layer terms at each of the boundary points is carried out independently of the layer terms at the other boundary point, without loss of generality, we assume throughout this section that

$$u_0(1,t) = g_1(t) \qquad \text{for } t \in [0,T], \tag{4.4}$$

which implies that there is no boundary layer at $x = 1$. To describe the boundary layer at $x = 0$ and the initial layer at $t = 0$, we shall employ the stretched variables $\xi := x/\varepsilon$ and $\tau := t/\varepsilon^2$.

4.1 *Solution near the boundary $x = 0$, boundary-layer functions*

In this subsection we construct boundary layer functions associated with the boundary $x = 0$; they use the stretched variable $\xi = x/\varepsilon$. Let $v_0(\xi,t) := \tilde{v}_0(\xi,t;0)$, and the functions $\tilde{v}_0(\xi,t;p)$ and $v_1(\xi,t)$ be solutions of the equations

$$-\frac{\partial^2 \tilde{v}_0}{\partial \xi^2} + \tilde{F}(0,t,\tilde{v}_0;p) = 0, \tag{4.5a}$$

$$-\frac{\partial^2 v_1}{\partial \xi^2} + v_1 F_s(0,t,v_0) = -\xi\, F_x\big(0,t,v_0\big), \tag{4.5b}$$

where $\xi > 0$, subject to the boundary conditions

$$\tilde{v}_0(0,t;p) = g_0(t) - u_0(0,t), \qquad v_1(0,t) = 0, \qquad \tilde{v}_0(\infty,t;p) = v_1(\infty,t) = 0. \tag{4.5c}$$

Note that the equation for $\tilde{v}_0$ is a nonlinear autonomous ordinary differential equation, while the equation for v_1 is a linear ordinary differential equation; in these equations, t and p appear as parameters. Note also that v_1 is not a perturbed function as it does not depend on p. Our conditions (A1), (A2) are precisely what is needed to ensure existence and asymptotic properties of $\tilde{v}_0$ and v_1. To be more specific, for the solvability and properties of the two problems described by (4.5) we have the following result.

LEMMA 4.1 Set $\gamma_L^2 = \min_{t\geqslant 0} f_u(0,t,u_0(0,t)) > \gamma^2$, where $\gamma > 0$ is from (A1). Then there is $p_0 \in (0,\gamma_L^2)$ such that for all $|p| \leqslant p_0$ there exist functions $\tilde{v}_0(\xi,t;p)$, $v_0(\xi,t)$ and $v_1(\xi,t)$ which satisfy (4.5). For $\tilde{v}_0$ and v_0 we have

$$v_0 \geqslant 0, \qquad |v_0 + \varepsilon v_1| \leqslant Ct, \qquad \frac{\partial \tilde{v}_0}{\partial p} \geqslant 0, \qquad \text{for all} \quad \xi, t \geqslant 0. \tag{4.6}$$

Furthermore, for any arbitrarily small but fixed $\delta \in (0, \gamma_L - \sqrt{p_0})$, there is a constant $\bar{C}_\delta$ such that

$$\Big|\frac{\partial^k \tilde{v}_0}{\partial \xi^k}\Big| + \Big|\frac{\partial^k v_1}{\partial \xi^k}\Big| + \Big|\frac{\partial^l \tilde{v}_0}{\partial t^l}\Big| + \Big|\frac{\partial^l v_1}{\partial t^l}\Big| + \Big|\frac{\partial \tilde{v}_0}{\partial p}\Big| \leqslant \bar{C}_\delta e^{-(\gamma_L - \sqrt{p_0} - \delta)\xi} \tag{4.7}$$

for $\xi, t \geqslant 0$ and $k = 0,\dots,4$, $l = 0,1,2$.

Proof. The existence and most of the properties of v_0 and $\tilde{v}_0$ follow from (Kopteva & Stynes, 2004, Lemma 2.3). For v_1, we use a result presented in (Fife, 1973, Lemma 2.2) and (Vasil'eva *et al.*, 1995, §2.3.1). In particular, to obtain estimates (4.7), one observes that the derivatives of $\tilde{v}_0$ and v_1 with respect to ξ and t, as well as $\partial\tilde{v}_0/\partial p$, all satisfy linear differential equations with the same differential operator, similar to the one in the equation (4.5b).

We especially elaborate on the proof of $|v_0 + \varepsilon v_1| \leqslant Ct$ as its analogues do not appear in the three cited publications. Recall the corner compatibility condition $g_0(0) - u_0(0,0) = 0$ from (3.2), which implies $|g_0(t) - u_0(0,t)| \leqslant Ct$. Combining this with $|v_0(\xi,t)| + |v_1(\xi,t)| \leqslant C|v_0(0,t)|$ (which follows from the cited analyses of v_0 and v_1) and $v_0(0,t) = g_0(t) - u_0(0,t)$, yields the desired estimate. □

For later purposes we shall now obtain two estimates that involve $\tilde{v}_0$, v_0 and v_1. The first estimate is concerned with the correction $v_0 + \varepsilon v_1$ to the reduced solution u_0 near $x = 0$. We claim that

$$\varepsilon^2\big[\tfrac{\partial}{\partial t} - \tfrac{\partial^2}{\partial x^2}\big](v_0 + \varepsilon v_1) + F(x,t,v_0 + \varepsilon v_1) = O(\varepsilon^2). \tag{4.8}$$

This immediately implies that $\mathcal{T}(u_0 + v_0 + \varepsilon v_1) = O(\varepsilon^2)$. Noting that $(u_0 + v_0 + \varepsilon v_1)\big|_{x=0} = g_0(t)$ and that $v_0 + \varepsilon v_1$ is decaying as $\xi \to \infty$, we now expect that $u_0 + v_0 + \varepsilon v_1$ approximates a solution u of our problem (1.1) near the boundary $x = 0$.

Estimate (4.8) is standard in the asymptotic analysis. It is obtained using $\varepsilon^2\big[\frac{\partial}{\partial t}-\frac{\partial^2}{\partial x^2}\big](v_0+\varepsilon v_1)=-\frac{\partial^2}{\partial\xi^2}(v_0+\varepsilon v_1)+O(\varepsilon^2)$. Combining this with (4.5a) and (4.5b), yields

$$\tfrac{\partial^2}{\partial\xi^2}(v_0+\varepsilon v_1)=F(0,t,v_0)+\varepsilon\xi\,F_x(0,t,v_0)+\varepsilon v_1\,F_s(0,t,v_0)=F(\varepsilon\xi,t,v_0+\varepsilon v_1)+O(\varepsilon^2).$$

Here we also used a Taylor series expansion of $F(\varepsilon\xi,t,v_0+\varepsilon v_1)$ in ε, in which the quadratic remainder terms are all $O(\varepsilon^2)$. To estimate the quadratic terms, we note that $|F_{xx}|\leqslant C|v_0+\varepsilon v_1|$ (which follows from (4.1)), $|F_{ss}|+|F_{xs}|\leqslant C$, and then $(\xi^2+1)(|v_0|+|v_1|)\leqslant C$ (which follows from (4.7)). Thus (4.8) is established.

Our second auxiliary estimate is for $\tilde v_0-v_0$:

$$\varepsilon^2[\tfrac{\partial}{\partial t}-\tfrac{\partial^2}{\partial x^2}](\tilde v_0-v_0)=-F(x,t,\cdot)\Big|_{v_0+\varepsilon v_1}^{\tilde v_0+\varepsilon v_1}+pv_0+O(\varepsilon^2+p^2). \tag{4.9}$$

It follows from $\varepsilon^2\big[\frac{\partial}{\partial t}-\frac{\partial^2}{\partial x^2}\big](\tilde v_0-v_0)=-\frac{\partial^2}{\partial\xi^2}(\tilde v_0-v_0)+O(\varepsilon^2)$ combined with (4.5a), which implies

$$\tfrac{\partial^2}{\partial\xi^2}(\tilde v_0-v_0)=F(0,t,\cdot)\Big|_{v_0}^{\tilde v_0}+p\tilde v_0=F(x,t,\cdot)\Big|_{v_0+\varepsilon v_1}^{\tilde v_0+\varepsilon v_1}-xF_x(\hat x,t,\cdot)\Big|_{v_0+\varepsilon\hat s}^{\tilde v_0+\varepsilon\hat s}-\varepsilon v_1\,F_s(\hat x,t,\cdot)\Big|_{v_0+\varepsilon\hat s}^{\tilde v_0+\varepsilon\hat s}+p\tilde v_0,$$

for some $\hat x\in(0,x)$ and $|\hat s|\leqslant|v_1|$ Recalling that $x=\varepsilon\xi$ and noting that, by the estimate for $\frac{\partial\tilde v_0}{\partial p}$ in (4.7), we have $(1+\xi)|\tilde v_0-v_0|=O(p)$, yields (4.9).

4.2 *Solution near $t=0$, initial-layer functions*

In this subsection we construct initial-layer functions to describe the solution near $t=0$; they use the stretched variable $\tau=t/\varepsilon^2$. Let $w_0(x,\tau):=\tilde w_0(x,\tau;0)$, and the function $\tilde w_0(x,\tau;p)$ be a solution of the initial-value problem

$$\frac{\partial\tilde w_0}{\partial\tau}=-\tilde F(x,0,\tilde w_0;p)\quad\text{for }\ \tau>0,\qquad \tilde w_0(x,0;p)=\varphi(x)-u_0(x,0). \tag{4.10a}$$

Since w_0 and $\tilde w_0$ describe a correction to $u_0(x,t)$ for small values of t, we look for a solution of (4.10a) that satisfies an additional condition

$$\tilde w_0(x,\infty;p)=0. \tag{4.10b}$$

Here $x\in[0,1]$ and p appear as parameters.

For each fixed x and p, problem (4.10) is a particular case of the auxiliary initial value problem

$$\tfrac{\mathrm d}{\mathrm d\tau}\omega=-\phi(\omega)\quad\text{for }\ \tau>0,\qquad \omega(0)=\omega_0\geqslant 0,\qquad \omega(\infty)=0, \tag{4.11}$$

for which we have the following result

LEMMA 4.2 Let a sufficiently smooth function ϕ satisfy

$$\phi(0)=0,\qquad \phi'(0)>0,\qquad \phi(s)>0\quad\text{for all }\ s\in(0,\omega_0]. \tag{4.12}$$

(i) Then problem (4.11) has a solution $0\leqslant\omega\leqslant\omega_0$, and for any arbitrarily small but fixed $\delta\in(0,\phi'(0))$, there is a constant $\bar C_\delta$ such that

$$|\omega|+|\omega'|+|\omega''|\leqslant\omega_0\,\bar C_\delta\,e^{-[\phi'(0)-\delta]\tau}\qquad\text{for }\ \tau\geqslant 0. \tag{4.13}$$

(ii) Set $\hat{\omega} := \omega/\omega_0$ if $\omega_0 > 0$, or $\hat{\omega} := e^{-\phi'(0)\tau}$ if $\omega_0 = 0$. Then the related linear problem

$$\tfrac{\mathrm{d}}{\mathrm{d}\tau}\chi + \chi\phi'(\omega) = \psi(\tau) \quad \text{for } \tau > 0, \qquad \chi(0) = \chi_0, \qquad \chi(\infty) = 0, \tag{4.14}$$

where $|\psi(\tau)| \leqslant C(1+\tau^m)\hat{\omega}(\tau)$ for some $m \geqslant 0$, has a solution such that $|\chi(\tau)| \leqslant C(\chi_0 + 1 + \tau^{m+1})\hat{\omega}(\tau)$. If we also have $\chi_0 = 0$ and $\psi \geqslant 0$, then $\chi \geqslant 0$ for all $\tau \geqslant 0$.

Proof. (i) If $\omega_0 = 0$, then $\omega(\tau) = 0$ for all τ and the assertion follows. Otherwise, if $\omega_0 > 0$, consider the phase plane (ω, ω') for the equation $\omega' = -\phi(\omega)$. By (4.12), there is a trajectory that leaves the point $(\omega_0, -\phi(\omega_0))$ and enters the point $(0,0)$, which is a fixed point for this equation. Furthermore, since $\phi(\omega) > 0$ for all $\omega \in (0, \omega_0]$, this entire trajectory will lie in the quarter plane $\{\omega > 0,\ \omega' < 0\}$; therefore the corresponding solution $\omega(\tau)$ is positive and decreasing to 0. It remains to show that the solution trajectory enters $(0,0)$ as $\tau \to \infty$, and also the exponential decay estimates (4.13). Note that for any $\delta \in (0, \phi'(0))$, there exists $s_\delta \in (0, \omega_0)$ such that $[\phi'(0) - \delta]s \leqslant \phi(s) \leqslant [\phi'(0) + \delta]s$ for all $s \in [0, s_\delta]$. Furthermore, there exists $\tau_\delta > 0$ such that $\omega(\tau_\delta) = s_\delta$ (otherwise, if $\omega(\tau) > s_\delta$ for all τ, then $\omega'(\tau) \leqslant -C$ for some positive constant C, which yields a contradiction $\omega(\infty) = -\infty$ with (4.11)). Thus for all $\tau \geqslant \tau_\delta$ we have $[\phi'(0) - \delta]\omega \leqslant \omega' \leqslant [\phi'(0) + \delta]\omega$, which implies that $e^{-[\phi'(0)+\delta]\tau} \leqslant \omega(\tau)/\omega(\tau_\delta) \leqslant e^{-[\phi'(0)-\delta]\tau}$ for $\tau \geqslant \tau_\delta$. The estimates for ω and ω' in (4.13) follow immediately as $\omega(\tau_\delta) < \omega_0$. Finally, the estimate for ω'' in (4.13) is obtained noting that $\omega'' = -\omega'\phi'(\omega)$.
(ii) To solve (4.14), note that the corresponding homogeneous equation $\frac{\mathrm{d}}{\mathrm{d}\tau}\theta + \theta\phi'(\omega) = 0$ has a positive solution θ such that $\theta(0) = 1$. If $\omega_0 > 0$, then we recall from part (i) that $\omega' < 0$ and $C^{-1} \leqslant |\omega'|/\omega \leqslant C$ and thus choose $\theta := \omega'/\omega'(0) > 0$ so that $C^{-1} \leqslant \theta/\hat{\omega} \leqslant C$; otherwise, if $\omega_0 = 0$ and thus $\omega = 0$, then, by (4.12), we have $\phi'(\omega) = \phi'(0) > 0$ and so choose $\theta(\tau) := e^{-\phi'(0)\tau} = \hat{\omega}$. Now, the unique solution of (4.14) is given by

$$\chi(\tau) = \chi_0\,\theta(\tau) + \theta(\tau)\int_0^\tau \frac{\psi(\tau')}{\theta(\tau')}\mathrm{d}\tau',$$

where $|\psi(\tau)| \leqslant C(1+\tau^m)\theta(\tau)$. The desired assertions follow. □

We now apply Lemma 4.2 to problem (4.10) as follows.

LEMMA 4.3 Set $\gamma_0^2 := \min\limits_{x\in[0,1]} f_u(x, 0, u_0(x,0)) > \gamma^2$, where $\gamma > 0$ is from (A1). Then there is $p_0 \in (0, \gamma_0^2)$ such that for all $|p| \leqslant p_0$, problem (4.10) has a solution $\tilde{w}_0(x, \tau; p)$. For $\tilde{w}_0$ and w_0 we have

$$0 \leqslant w_0 \leqslant Cx, \qquad \frac{\partial \tilde{w}_0}{\partial p} \geqslant 0, \qquad \text{for all} \quad x \in [0,1],\ \tau \geqslant 0. \tag{4.15}$$

Furthermore, for any arbitrarily small but fixed $\delta \in (0, \gamma_0^2 - p_0)$, there is a constant $\bar{C}_\delta$ such that

$$\left|\frac{\partial^l \tilde{w}_0}{\partial \tau^l}\right| + \left|\frac{\partial^k \tilde{w}_0}{\partial x^k}\right| + \left|\frac{\partial \tilde{w}_0}{\partial p}\right| \leqslant \bar{C}_\delta e^{-(\gamma_0^2 - p_0 - \delta)\tau}. \tag{4.16}$$

for $x \in [0,1]$, $\tau \geqslant 0$ and $k = 0, \dots, 4$, $l = 0, 1, 2$.

Proof. For each fixed x and p, problem (4.10) is a particular case of the auxiliary problem (4.11) with a solution $\omega := \tilde{w}_0$, the initial condition $\omega_0 := \varphi(x) - u_0(x,0)$, and the right-hand side function $\phi(s) := \tilde{F}(x, 0, s; p) = f(x, 0, u_0(x,0) + s) - ps$, for which we have $\phi'(s) = f_u(x, 0, u_0(x,0) + s) - p$. Note that (A1) implies that $\phi(0) = 0$ and $\phi'(0) \geqslant \gamma_0^2 - |p| > 0$, while (A3) combined with (3.1) yields $\phi(s) > 0$ for all $s \in (0, \omega_0]$ provided that p_0 is chosen sufficiently small. Thus the hypotheses (4.12) of

Lemma 4.2 are satisfied. Now Lemma 4.2(i) implies existence of a solution $0 \leqslant \tilde{w}_0 \leqslant \varphi(x) - u_0(x,0)$ and the estimates for $\frac{\partial^l}{\partial \tau^l}\tilde{w}_0$, where $l = 0,1,2$, in (4.16). Next, the bound $0 \leqslant w_0 \leqslant Cx$ in (4.15) is obtained from $w_0 = \tilde{w}_0\big|_{p=0}$ and $0 \leqslant \tilde{w}_0 \leqslant \varphi(x) - u_0(x,0)$, noting that the corner compatibility condition $\varphi(0) - u_0(0,0) = 0$ from (3.2) implies $\varphi(x) - u_0(x,0) \leqslant Cx$.

It remains now to estimate the functions $\frac{\partial}{\partial p}\tilde{w}_0$ and $\frac{\partial^k}{\partial x^k}\tilde{w}_0$ for $k = 1,\ldots,4$. Differentiating the equation in (4.10a) with respect to p, or k times with respect to x, we see that these functions are solutions of the initial value problem (4.14) with $\phi'(\omega) = \phi'(\tilde{w}_0) = \tilde{F}_s(x,0,\tilde{w}_0)$ and various right-hand sides and initial data. In particular, we have $\psi := \tilde{w}_0$ and $\chi_0 := 0$ for $\chi = \frac{\partial}{\partial p}\tilde{w}_0$, which, by Lemma 4.2(ii), implies that $\frac{\partial}{\partial p}\tilde{w}_0 \geqslant 0$ and the estimate for this function in (4.16). Furthermore, for $\chi = \frac{\partial}{\partial x}\tilde{w}_0$ we use $\psi := -\tilde{F}_x(x,0,\tilde{w}_0)$ (for which we have $|\psi| \leqslant C\tilde{w}_0$, by (4.1)) and $\chi_0 := \varphi'(x) - u_{0,x}(x,0)$; now the estimate for $\frac{\partial}{\partial x}\tilde{w}_0$ in (4.16) is obtained by again applying Lemma 4.2(ii). The remaining bounds in (4.16) are obtained similarly, by evaluating the functions ψ and χ_0 corresponding to $\chi = \frac{\partial^k}{\partial x^k}\tilde{w}_0$ with $k > 1$, and then applying Lemma 4.2(ii). □

For later purposes we shall now obtain two estimates that involve $\tilde{w}_0$ and w_0. The first estimate is concerned with the correction w_0 to the reduced solution u_0 near $t = 0$. We claim that

$$\varepsilon^2\big[\tfrac{\partial}{\partial t} - \tfrac{\partial^2}{\partial x^2}\big]w_0 + F(x,t,w_0) = O(\varepsilon^2). \tag{4.17}$$

This immediately implies that $\mathcal{T}(u_0 + w_0) = O(\varepsilon^2)$. Noting that $(u_0 + w_0)\big|_{t=0} = \varphi(x)$ and that w_0 is decaying as $\tau \to \infty$, we expect that $u_0 + w_0$ approximates a solution u of our problem (1.1) near $t = 0$.

Estimate (4.17) is standard in asymptotic analysis. It is obtained noting that $\varepsilon^2\big[\frac{\partial}{\partial t} - \frac{\partial^2}{\partial x^2}\big]w_0 = \frac{\partial}{\partial \tau}w_0 + O(\varepsilon^2)$ and then recalling (4.10a), which yields $\frac{\partial}{\partial \tau}w_0 = -F(x,0,w_0) = -F(x,t,w_0) + O(\varepsilon^2)$. Here we also used a Taylor series expansion of $F(x,t,w_0)$ in t. The linear remainder term $tF_t(x,\hat{t},w_0)$, for some $\hat{t} \in (0,t)$, was estimated combining $t = \varepsilon^2\tau$ with $|F_t| \leqslant Cw_0$ (which follows from (4.1)) and then invoking (4.16). Thus (4.17) is established.

Our second auxiliary estimate is for $\tilde{w}_0 - w_0$:

$$\varepsilon^2[\tfrac{\partial}{\partial t} - \tfrac{\partial^2}{\partial x^2}](\tilde{w}_0 - w_0) = -F(x,t,\cdot)\Big|_{w_0}^{\tilde{w}_0} + pw_0 + O(\varepsilon^2 + p^2). \tag{4.18}$$

It follows from $\varepsilon^2\big[\frac{\partial}{\partial t} - \frac{\partial^2}{\partial x^2}\big](\tilde{w}_0 - w_0) = \frac{\partial}{\partial \tau}(\tilde{w}_0 - w_0) + O(\varepsilon^2)$ combined with (4.10a), which implies

$$\tfrac{\partial}{\partial t}(\tilde{w}_0 - w_0) = -F(x,0,\cdot)\Big|_{w_0}^{\tilde{w}_0} + p\tilde{w}_0 = -F(x,t,\cdot)\Big|_{w_0}^{\tilde{w}_0} + tF_t(x,\hat{t},\cdot)\Big|_{w_0}^{\tilde{w}_0} + p\tilde{w}_0,$$

for some $\hat{t} \in (0,t)$. Recalling that $t = \varepsilon^2\tau$ and noting that, by the bound for $\frac{\partial \tilde{w}_0}{\partial p}$ in (4.16), we have $(1+\tau)|\tilde{w}_0 - w_0| = O(p)$, yields (4.18).

REMARK 4.4 Assumption (A3) is necessary for existence of the initial-layer functions w_0 and $\tilde{w}_0$, which are solutions of problem (4.10). To understand this assertion, note that (4.10) is a particular case of problem (4.11), and assumption (A3) for problem (4.10) is equivalent to the condition $\phi(s) > 0$ for all $s \in (0,\omega_0]$, which appears in (4.12). Now, if $|\phi'(s)| \leqslant C$ for all $s \in [0,\omega_0]$, then our conditions (4.12), with $\phi'(0) > 0$ relaxed to $\phi'(0) \geqslant 0$, are necessary for problem (4.11) having a solution. (This can be shown extending the phase plane analysis used in the proof of Lemma 4.2.)

4.3 *First-order asymptotic expansion*

In the previous subsections we have defined the boundary-layer functions v_0 and v_1 and the initial-layer function w_0. In this subsection, these functions and the reduced solution u_0 are assembled in the following first-order asymptotic expansion for our problem (1.1):

$$u_{\rm as}(x,t) := u_0(x,t) + [\,v_0(\xi,t) + \varepsilon v_1(\xi,t)\,] + w_0(x,\tau). \tag{4.19}$$

Note that no corner functions are needed in the above asymptotic expansion due to the compatibility conditions (3.2). Indeed, examining problems (4.5) for v_0 and v_1, in view of (3.2) with $l = 0$, yields $v_0(\xi,0) = v_1(\xi,0) = 0$ for all $\xi \geqslant 0$; similarly, examining problem (4.10) for w_0 in view of (3.2), yields $w_0(0,\tau) = w_0(1,\tau) = 0$ for all $\tau \geqslant 0$. Therefore, we get

$$u_{\rm as}(x,0) = \varphi(x), \qquad u_{\rm as}(0,t) = g_0(t), \qquad u_{\rm as}(1,t) = g_1(t) + O(\varepsilon^2), \tag{4.20}$$

or in other words, $u_{\rm as}(x,0) = u(x,0)$ and $|u_{\rm as}(l,t) - u(l,t)| = O(\varepsilon^2)$ at the boundary points $l = 0, 1$. It should be noted that the last relation in (4.20) follows from $u_{\rm as}(1,t) = u_0(1,t) + (v_0 + \varepsilon v_1)\big|_{\xi=1/\varepsilon}$ combined with our assumption (4.4) and the estimate $|v_0 + \varepsilon v_1| \leqslant C_\delta e^{-(\gamma_L-\delta)/\varepsilon} \leqslant C\varepsilon^2$ for $\xi = 1/\varepsilon$, for which we invoked (4.7).

Furthermore, we have the following standard result for $\mathcal{T}u_{\rm as}$.

LEMMA 4.5 The asymptotic expansion $u_{\rm as}$ from (4.19) satisfies $\mathcal{T}u_{\rm as} = O(\varepsilon^2)$.

Proof. First we combine $\varepsilon^2\big[\frac{\partial}{\partial t} - \frac{\partial^2}{\partial x^2}\big]u_0 = O(\varepsilon^2)$ with (4.8) and (4.17) and, using notation (4.2), get

$$\mathcal{T}u_{\rm as} = \varepsilon^2\big[\tfrac{\partial}{\partial t} - \tfrac{\partial^2}{\partial x^2}\big]u_{\rm as} + F(x,t,v_0+\varepsilon v_1 + w_0) = F(x,t,\cdot)\Big|_{v_0+\varepsilon v_1;\; w_0}^{(v_0+\varepsilon v_1)+w_0} + O(\varepsilon^2).$$

By (4.3), this yields

$$|\mathcal{T}u_{\rm as}| \leqslant C\,|(v_0+\varepsilon v_1)w_0| + O(\varepsilon^2) \leqslant C\,t\,e^{-(\gamma_0^2-\delta)\tau} + O(\varepsilon^2) \leqslant C\varepsilon^2.$$

Here we estimated $|v_0 + \varepsilon v_1|$ using (4.6) and w_0 using (4.16), and also invoked $t = \varepsilon^2\tau$. □

4.4 *Modified asymptotic expansion, existence of a solution between upper and lower solutions*

In this section we construct upper and lower solutions, and therefore, prove an existence of a solution in an $O(\varepsilon^2)$ neighbourhood of our asymptotic expansion. The upper and lower solutions are obtained by perturbing our asymptotic expansion (4.19), in which we replace the boundary- and initial-layer functions v_0 and w_0 by their perturbed versions $\tilde v_0$ and $\tilde w_0$, and then add the term $C_0 p$, as follows:

$$\beta(x,t;p) := u_0(x,t) + [\,\tilde v_0(\xi,t;p) + \varepsilon v_1(\xi,t)\,] + \tilde w_0(x,\tau;p) + C_0 p. \tag{4.21}$$

Occasionally we shall use an alternative equivalent representation

$$\beta(x,t;p) = u_{\rm as} + V + W + C_0 p, \qquad \text{where} \quad V := \tilde v_0 - v_0, \quad W := \tilde w_0 - w_0. \tag{4.22}$$

Note that for V and W here, by the estimates for $\frac{\partial}{\partial p}\tilde v_0$ and $\frac{\partial}{\partial p}\tilde w_0$ in (4.7) and (4.16), we get

$$(1+\xi)|V| \leqslant Cp, \qquad (1+\tau)|W| \leqslant Cp. \tag{4.23}$$

LEMMA 4.6 For the function $\beta(x,t;p)$ of (4.21) we have $\beta = u_{\rm as} + O(p)$. Furthermore, if $p \geqslant 0$, then

$$\beta(x,t;-p) \leqslant u_{\rm as} - C_0 p \leqslant u_{\rm as} + C_0 p \leqslant \beta(x,t;p) \qquad \text{for all } (x,t) \in [0,1]\times[0,T]. \tag{4.24}$$

Proof. The first assertion immediately follows from (4.22) and (4.23). Noting that $u_{\rm as}(x,t) = \beta(x,t;0)$ and then recalling the bounds $\partial\tilde v_0/\partial p \geqslant 0$ and $\partial\tilde w_0/\partial p \geqslant 0$ from (4.6) and (4.15), yields the second assertion (4.24). □

Furthermore, for $\mathcal{T}\beta$ we get the following result.

LEMMA 4.7 For all $(x,t) \in (0,1)\times(0,T]$ we have

$$\mathcal{T}\beta = C_0 p f_u(x,t,u_0) + p\,[1 + C_0\lambda](v_0 + w_0) + O(\varepsilon^2 + p^2),$$

where $\lambda = \lambda(x,t) := f_{uu}(x,t,u_0 + \vartheta[v_0 + w_0])$ for some $\vartheta = \vartheta(x,t) \in (0,1)$.

Proof. By Lemma 4.5, we have $\mathcal{T}u_{\rm as} = O(\varepsilon^2)$. Thus it suffices to investigate $\mathcal{T}\beta - \mathcal{T}u_{\rm as}$, for which, by (4.22), we have

$$\mathcal{T}\beta - \mathcal{T}u_{\rm as} = \varepsilon^2\big[\tfrac{\partial}{\partial t} - \tfrac{\partial^2}{\partial x^2}\big](V+W) + f(x,t,\cdot)\Big|_{u_{\rm as}}^{\beta}. \tag{4.25}$$

Now, recalling (4.9) and (4.18) yields

$$\varepsilon^2[\tfrac{\partial}{\partial t} - \tfrac{\partial^2}{\partial x^2}](V+W) = -F(x,t,\cdot)\Big|_{v_0+\varepsilon v_1}^{\tilde v_0+\varepsilon v_1} - F(x,t,\cdot)\Big|_{w_0}^{\tilde w_0} + p[v_0 + w_0] + O(\varepsilon^2 + p^2),$$

and therefore, using Taylor series expansions combined with $V^2 + W^2 \leqslant Cp^2$ (see (4.23)), we get

$$\varepsilon^2[\tfrac{\partial}{\partial t} - \tfrac{\partial^2}{\partial x^2}](V+W) = -VF_s(x,t,v_0+\varepsilon v_1) - WF_s(x,t,w_0) + p(v_0+w_0) + O(\varepsilon^2 + p^2). \tag{4.26}$$

Similarly, we obtain

$$\begin{aligned} f(x,t,\cdot)\Big|_{u_{\rm as}}^{u_{\rm as}+V+W} &= F(x,t,\cdot)\Big|_{v_0+\varepsilon v_1+w_0}^{v_0+\varepsilon v_1+w_0+V+W} = [V+W]F_s(x,t,v_0+\varepsilon v_1+w_0) + O(p^2) \\ &= VF_s(x,t,v_0+\varepsilon v_1) + WF_s(x,t,w_0) + O(|Vw_0| + |W(v_0+\varepsilon v_1)| + p^2). \end{aligned} \tag{4.27}$$

Next, note that invoking $\varepsilon v_1 + (V+W) = O(\varepsilon + p)$, we get

$$\begin{aligned} f(x,t,\cdot)\Big|_{u_{\rm as}+V+W}^{\beta} &= f(x,t,\cdot)\Big|_{u_{\rm as}+V+W}^{u_{\rm as}+V+W+C_0p} = C_0 p\,[f_u(x,t,u_0+v_0+w_0) + O(\varepsilon + p)] \\ &= C_0 p\,[f_u(x,t,u_0) + \lambda(v_0+w_0)] + O(\varepsilon^2 + p^2), \end{aligned} \tag{4.28}$$

where $\lambda = \lambda(x,t) := f_{uu}(x,t,u_0 + \vartheta[v_0 + w_0])$ for some $\vartheta = \vartheta(x,t) \in (0,1)$.

Combining relations (4.25), (4.26), (4.27), (4.28) with $\mathcal{T}u_{\rm as} = O(\varepsilon^2)$, we arrive at

$$\mathcal{T}\beta = C_0 p f_u(x,t,u_0) + p\,[1 + C_0\lambda](v_0+w_0) + O(|Vw_0| + |W(v_0+\varepsilon v_1)|) + O(\varepsilon^2 + p^2).$$

The desired assertion follows by invoking $|Vw_0| + |W(v_0+\varepsilon v_1)| \leqslant C(x|V| + t|W|) = O(\varepsilon p)$. Here we estimated $|w_0|$ and $|v_0 + \varepsilon v_1|$ using (4.15) and (4.6), and then combined $x = \varepsilon\xi$ and $\tau = \varepsilon^2\tau$ with $\xi|V| \leqslant Cp$ and $\tau|W| \leqslant Cp$ from (4.23). □

COROLLARY 4.8 There are $C_0 > 0$ and $C_1 > 0$ such that for all $|p| \leqslant p_0$ we have

$$\begin{array}{rcll} \mathcal{T}\beta & \geqslant & C_0 p\gamma^2 - C_1(\varepsilon^2 + p^2), & \text{if} \quad p > 0, \\ \mathcal{T}\beta & \leqslant & -C_0|p|\gamma^2 + C_1(\varepsilon^2 + p^2), & \text{if} \quad p < 0. \end{array}$$

Proof. Recall (A1) and the estimates $v_0 \geqslant 0$, $w_0 \geqslant 0$ from (4.6), (4.15). Now choose C_0 so that $1 + C_0\lambda \geqslant 0$ for all x and t. This is possible to do because $|\lambda(x,t)| \leqslant C$. □

Now we are ready to establish existence of a unique solution of (1.1) that lies in an $O(\varepsilon^2)$ neighbourhood of our asymptotic expansion.

THEOREM 4.9 There is a sufficiently small $\varepsilon_0 > 0$ such that for all $\varepsilon \leqslant \varepsilon_0$, there exists a unique solution u of problem (1.1). Furthermore, for this solution we have $|u(x,t) - u_{\text{as}}(x,t)| \leqslant C\varepsilon^2$ for all $(x,t) \in [0,1] \times [0,T]$.

Proof. Set $\bar{p} = C_2\varepsilon^2$, where $C_2 \geqslant 2C_1/(C_0\gamma^2)$ so that $C_0\bar{p}\gamma^2 \geqslant 2C_1\varepsilon^2$. Then, by Corollary 4.8, for $\varepsilon \leqslant 1/C_2$ we get $\bar{p} \leqslant \varepsilon$ so $C_1(\varepsilon^2 + p^2) \leqslant 2C_1\varepsilon^2$ and therefore

$$\mathcal{T}\beta(x,t;-\bar{p}) \leqslant 0 \leqslant \mathcal{T}\beta(x,t;\bar{p}). \tag{4.29a}$$

Furthermore, in view of (4.24), choosing C_2 sufficiently large so that $C_0\bar{p} = C_0C_2\varepsilon^2$ dominates the term $O(\varepsilon^2)$ in (4.20), yields

$$\beta(x,0;-\bar{p}) \leqslant \varphi(x) \leqslant \beta(x,0;\bar{p}), \qquad \beta(l,t;-\bar{p}) \leqslant g_l(t) \leqslant \beta(l,t;\bar{p}) \quad \text{for } l = 0, 1. \tag{4.29b}$$

By (4.24), we also have

$$\beta(x,t;-\bar{p}) \leqslant \beta(x,t;\bar{p}). \tag{4.29c}$$

Comparing (4.29) with (1.1), we see that $\beta(x,t;-\bar{p})$ and $\beta(x,t;\bar{p})$ are ordered lower and upper solutions, respectively, for problem (1.1) (sometimes they are called ordered sub- and super-solutions); see Pao (1992). Now, applying (Pao, 1992, Theorem 5.1) yields existence of a solution u between $\beta(x,t;-\bar{p})$ and $\beta(x,t;\bar{p})$:

$$\beta(x,t;-\bar{p}) \leqslant u(x,t) \leqslant \beta(x,t;\bar{p}).$$

Furthermore, Proposition 2.1 implies that this is a unique solution. Since, by Lemma 4.6, we have $\beta(x,t;\pm\bar{p}) = u_{\text{as}} + O(\bar{p}) = u_{\text{as}} + O(\varepsilon^2)$, then $|u - u_{\text{as}}| \leqslant C\varepsilon^2$. □

REMARK 4.10 We have established existence of a solution u of problem (1.1) for sufficiently small values of ε such that $\varepsilon \leqslant \varepsilon_0$. Note that the theory of lower and upper solutions also applies to the case of $\varepsilon \in (\varepsilon_0, 1]$, when ε is not small. But the construction of lower and upper solutions for this case cannot any longer invoke asymptotic expansions, and will depend on a particular nonlinear function f in (1.1a).

5. Analysis of the numerical method

In this section we investigate the numerical method (2.1); note that our results also apply to a more conventional numerical method (1.3) as it is a particular case of (2.1) with $\hat{C} = 0$.

We make a further simplifying assumption to facilitate our presentation. Throughout this section we take

$$\varepsilon \leqslant C(N^{-1} + M^{-1/2}). \tag{5.1}$$

This is not a practical restriction, and from a theoretical viewpoint the analysis of a nonlinear problem such as (1.1) would be very different if ε were not small. Furthermore, by invoking higher-order asymptotic expansions (compared to (4.19)), condition (5.1) can be relaxed to $\varepsilon \leqslant C(N^{-\delta} + M^{-\delta/2})$ for any arbitrarily small but fixed $\delta \in (0,1]$.

5.1 *Layer-adapted meshes, truncation error*

We shall consider discrete problems (1.3) and (2.1) on two popular layer-adapted meshes, which have been shown to yield convergence of various numerical methods uniformly with respect to the the singular perturbation parameter(s). The meshes are presented for the general case when the solution of problem (1.1) has boundary layers both at $x=0$ and $x=1$ and also an initial layer at $t=0$; see Figure 2. For convenience, we nevertheless continue our analysis in this section under assumption (4.4).

5.1 (a) Bakhvalov mesh first appeared in Bakhvalov (1969); we also refer the reader to Roos *et al.* (2008). The mesh points (x_i,t_j) are defined as $x_i = x(i/N)$ and $t_j = t(j/M)$, where the mesh-generating functions $x(\cdot),\, t(\cdot) \in C[0,1]$ are given by

$$x(\xi)=\begin{cases} \frac{2\varepsilon}{\gamma}\ln\frac{1}{1-4\xi} & \text{for} \quad \xi\in[0,\theta],\\ \frac12-d(\frac12-\xi) & \text{for} \quad \xi\in(\theta,\frac12],\\ 1-x(1-\xi) & \text{for} \quad \xi\in(\frac12,1],\end{cases} \qquad t(\eta)=\begin{cases} \frac{\varepsilon^2}{\gamma^2}\ln\frac{1}{1-2\eta} & \text{for} \quad \eta\in[0,\theta_0],\\ T-d_0(1-\eta) & \text{for} \quad \eta\in(\theta_0,1].\end{cases}$$

Here $\theta = 1/4 - C_3\varepsilon$ and $\theta_0 = 1/2 - C_4\varepsilon^2$ for some positive constants C_3 and C_4; and d and d_0 are chosen so that $x(\xi)$ and $t(\eta)$ are continuous at $\xi=\theta$ and $\eta=\theta_0$ respectively. These definitions of $x(\xi)$ and $t(\eta)$ are valid only for $\varepsilon \leqslant \frac18\min\{\gamma, 2C_3^{-1}\}$ and $\varepsilon^2 \leqslant \frac12\min\{\gamma^2 T, C_4^{-1}\}$, respectively, which is not a practical restriction (otherwise, we set $x(\xi)=\xi$ and/or $t(\eta)=T\eta$ and get a uniform mesh in the x- and/or t-direction). Note also that for a certain choice of C_3 and C_4, one obtains the original Bakhvalov mesh, for which $x(\cdot),\, t(\cdot)\in C^1[0,1]$.

5.1 (b) Shishkin mesh; see Shishkin (1992); Miller *et al.* (1996). This mesh is constructed as follows. Let $N/4$ and $M/2$ be positive integers and set

$$\sigma := \min\{\tfrac{2\varepsilon}{\gamma}\ln N,\ \tfrac14\}, \qquad \sigma_0 := \min\{\tfrac{\varepsilon^2}{\gamma^2}\ln M,\ \tfrac{T}{2}\}. \tag{5.2}$$

Now the piecewise uniform mesh $\{x_i\}_{i=0}^N$ is obtained by dividing the intervals $[0,\sigma]$, $[\sigma,1-\sigma]$ and $[1-\sigma,1]$ into $N/4$, $N/2$ and $N/4$ equidistant subintervals, respectively. Similarly the piecewise uniform mesh $\{t_j\}_{j=0}^M$ is obtained by dividing each of the intervals $[0,\sigma_0]$ and $[\sigma_0,T]$ into $M/2$ equidistant subintervals. In practice, one usually has $\sigma \ll 1$ and $\sigma_0 \ll 1$, so the x-mesh is coarse on $[\sigma,1-\sigma]$ and fine otherwise, while the t-mesh is coarse on $[\sigma_0,T]$ and fine on $[0,\sigma_0]$.

For the truncation error $\hat{\mathfrak{T}}^h\beta - \mathfrak{T}\beta$ of $\hat{\mathfrak{T}}^h$ from (2.1) on these meshes we have the following estimate.

LEMMA 5.1 Let $\beta(x,t)=\beta(x,t;p)$ be defined by (4.21), and let the mesh $\{(x_i,t_j)\}$ be either the Bakhvalov mesh of §5.1(a), or the Shishkin mesh of §5.1(b). Then for all $|p|\leqslant p_0$, where p_0 is a sufficiently small constant, we have

$$|\hat{\mathfrak{T}}^h\beta(x_i,t_j;p) - \mathfrak{T}\beta(x_i,t_j;p)| \leqslant C(N^{-2}\ln^{2m}N + M^{-1}\ln^m M),$$

where $m=0$ for the Bakhvalov mesh (a) and $m=1$ for the Shishkin mesh (b).

Proof. Choose p_0 in Lemmas 4.1 and 4.3 sufficiently small so that $\gamma_L - \sqrt{p_0} > \gamma$ and $\gamma_0^2 - p_0 > \gamma^2$; next, choose δ in (4.7) and (4.16) sufficiently small so that $\gamma_L - \sqrt{p_0} - \delta \geqslant \gamma$ and $\gamma_0^2 - p_0 - \delta \geqslant \gamma^2$.

Now, note that $\hat{\mathfrak{T}}^h\beta - \mathfrak{T}\beta = [\hat\varepsilon^2\delta_t - \varepsilon^2\frac{\partial}{\partial t}]\tilde w_0 - \varepsilon^2[\delta_x^2 - \frac{\partial^2}{\partial x^2}](\tilde v_0 + \varepsilon v_0) + O(\varepsilon^2)$. By (4.7), imitating the arguments in (Kopteva & Stynes, 2004, §3.4), we get $\varepsilon^2[\delta_x^2 - \frac{\partial^2}{\partial x^2}](\tilde v_0 + \varepsilon v_0) = O(N^{-2}\ln^{2m}N)$. In view of (5.1), to establish the desired estimate it now remains to show that

$$R_1 := \varepsilon^2[\delta_t - \tfrac{\partial}{\partial t}]\tilde w_0 = O(M^{-1}\ln^m M), \qquad R_2 := (\hat\varepsilon^2 - \varepsilon^2)\delta_t\tilde w_0 = O(M^{-1}\ln^m M). \tag{5.3}$$

Let $M_j^{(l)} := \max_{(x,t)\in[0,1]\times[t_{j-1},t_j]} |\frac{\partial^l}{\partial t^l}\tilde{w}_0|$. Taylor series expansions yield $|R_1| \leqslant C\varepsilon^2 \min\{k_j M_j^{(2)}, M_j^{(1)}\}$; similarly, we get $|R_2| \leqslant C(\hat{\varepsilon}_j^2 - \varepsilon^2)k_j^{-1}M_j^{(0)}$. Note that, by (4.16), here we have $M_j^{(l)} \leqslant C\varepsilon^{-2l}e^{-\gamma^2 t_{j-1}/\varepsilon^2}$ as $\frac{\partial^l}{\partial t^l} = \varepsilon^{-2l}\frac{\partial^l}{\partial \tau^l}$. Therefore

$$|R_1| \leqslant C\min\{\frac{k_j}{\varepsilon^2}, 1\}e^{-\gamma^2 t_{j-1}/\varepsilon^2}, \qquad |R_2| \leqslant C\max\{0, \hat{C} - \frac{\varepsilon^2}{k_j}\}e^{-\gamma^2 t_{j-1}/\varepsilon^2}. \tag{5.4}$$

We shall show that (5.4) implies (5.3) for the Bakhvalov mesh (a) and the Shishkin mesh (b) separately.

(a) Case 1: $\frac{j}{M} \leqslant \theta_0 - C_5M^{-1}$ for some $C_5 \geqslant 1$. Then we have $k_j \leqslant M^{-1}t'(\frac{j}{M}) = M^{-1}\frac{\varepsilon^2}{\gamma^2}[\frac{1}{2} - \frac{j}{M}]^{-1}$ and $e^{-\gamma^2 t_{j-1}/\varepsilon^2} = [1 - 2\frac{(j-1)}{M}]$, which imply

$$|R_1| \leqslant CM^{-1}\frac{1 - 2\frac{(j-1)}{M}}{\frac{1}{2} - \frac{j}{M}} = CM^{-1}2\Big(1 + \frac{M^{-1}}{\frac{1}{2} - \frac{j}{M}}\Big) \leqslant CM^{-1}.$$

Here we used $\frac{1}{2} - \frac{j}{M} \geqslant C_5M^{-1}$, which follows from $\theta_0 - \frac{j}{M} \geqslant C_5M^{-1}$. Furthermore, choosing $C_5 = C_5(\hat{C})$ sufficiently large, we obtain $\hat{C}k_j \leqslant \varepsilon^2$, which yields $R_2 = 0$.

Case 2: $\frac{j}{M} > \theta_0 - C_5M^{-1} = \frac{1}{2} - C_4\varepsilon^2 - C_5M^{-1}$. Now, a calculation shows that $t_{j-1} = t(\frac{j-1}{M}) \geqslant \frac{\varepsilon^2}{\gamma^2}\ln(\frac{1}{2}[C_4\varepsilon^2 + (C_5+1)M^{-1}]^{-1})$ and thus $e^{-\gamma^2 t_{j-1}/\varepsilon^2} \leqslant C(\varepsilon^2 + M^{-1})$. Combining this with $\min\{\frac{k_j}{\varepsilon^2}, 1\} \leqslant C\varepsilon^{-2}\min\{M^{-1}, \varepsilon^2\}$ yields the first desired bound $|R_1| \leqslant CM^{-1}$. As $\hat{C} - \varepsilon^2 k_j^{-1} > 0$ implies $\varepsilon^2 \leqslant CM^{-1}$, we also get the other desired bound $|R_2| \leqslant CM^{-1}$.

(b) For $j \leqslant M/2$ we have $k_j = C\varepsilon^2M^{-1}\ln M$, which implies $R_1 \leqslant CM^{-1}\ln M$ and $R_2 \leqslant CM^{-1}\ln M$ (as in this case $\hat{C} - \frac{\varepsilon^2}{k_j} \leqslant C\frac{k_j}{\varepsilon^2} \leqslant CM^{-1}\ln M$). Otherwise, for $j > M/2$, we get $e^{-\gamma^2 t_{j-1}/\varepsilon^2} \leqslant e^{-\gamma^2\sigma_0/\varepsilon^2} = M^{-1}$ and thus $|R_1| \leqslant CM^{-1}$ and $|R_2| \leqslant CM^{-1}$. □

5.2 *Existence and accuracy, discrete upper and lower solutions*

To establish existence of solutions of semilinear discrete equations (1.3) and (2.1), we invoke the theory of discrete upper and lower solutions outlined in the following result.

PROPOSITION 5.2 Assume that on an arbitrary mesh $\{(x_i, t_j)\}$ there exist discrete functions α and β such that $\alpha_{ij} \leqslant \beta_{ij}$ and

$$\hat{\mathfrak{T}}^h\alpha_{ij} \leqslant 0 \leqslant \hat{\mathfrak{T}}^h\beta_{ij}, \quad \alpha_{i,0} \leqslant \varphi(x_i) \leqslant \beta_{i,0}, \quad \alpha_{0,j} \leqslant g_0(t_j) \leqslant \beta_{0,j}, \quad \alpha_{N,j} \leqslant g_1(t_j) \leqslant \beta_{N,j},$$

where $i = 1, \ldots, N-1$, $j = 1, \ldots, M$. Then problem (2.1) has a solution $\hat{U}_{ij}$ such that $\alpha_{ij} \leqslant \hat{U}_{ij} \leqslant \beta_{ij}$.

Proof. The desired result is obtained imitating the proof of (Pao, 1985, Theorem 3.1) (where the case of $\hat{\varepsilon}_j = \varepsilon = 1$ was considered). It is crucial in this argument that the discrete operator $\hat{\mathfrak{T}}^h + CI$ satisfies the discrete maximum principle, where I is the identity operator and C is an arbitrarily large but fixed positive constant. Alternatively, one can get the assertion of this proposition noting that the mapping $\mathfrak{T}^h\colon \mathbb{R}^{(N+1)+(M+1)} \to \mathbb{R}^{(N+1)+(M+1)}$ is a Z-field; see Lorenz (1981); Kopteva & Stynes (2004). □

REMARK 5.3 The functions α and β of Proposition 5.2 are called ordered discrete lower and upper solutions (or sub- and super-solutions) of the discrete problem (2.1).

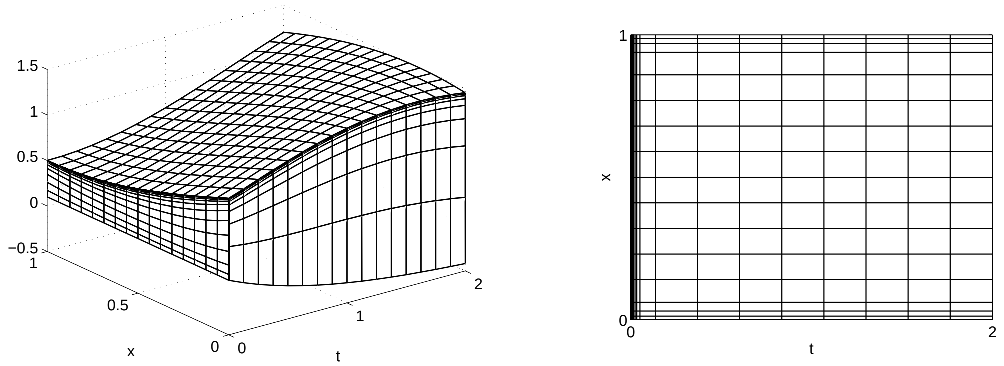

FIG. 2. Solution of test problem (6.1) for $\varepsilon = 10^{-4}$ (left); a layer-adapted mesh with $N = M = 16$ (right).

Now we are prepared to state existence of our discrete solutions and estimate their errors.

THEOREM 5.4 Let the mesh $\{(x_i,t_j)\}$ be either the Bakhvalov mesh of §5.1(a), or the Shishkin mesh of §5.1(b). Then for N and M sufficiently large independently of ε, there exist solutions U_{ij} and $\hat{U}_{ij}$ of discrete problems (1.3) and (2.1), respectively, such that their bilinear interpolants U^I and $\hat{U}^I$ satisfy

$$\begin{aligned} |U^I(x,t) - u(x,t)| &\leqslant C(N^{-2}\ln^{2m}N + M^{-1}\ln^m M), \\ |\hat{U}^I(x,t) - u(x,t)| &\leqslant C(N^{-2}\ln^{2m}N + M^{-1}\ln^m M), \end{aligned}$$

for all $(x,t) \in [0,1]\times[0,T]$, where u is the unique solution of problem (1.1), while $m = 0$ for the Bakhvalov mesh (a) and $m = 1$ for the Shishkin mesh (b).

Proof. As problem (1.3) is a particular case of problem (2.1), it suffices to prove the desired assertions only for $\hat{U}_{ij}$. Set $\bar{p} = C_6(N^{-2}\ln^{2m}N + M^{-1}\ln^m M)$ and choose C_6 sufficiently large so that, invoking Lemma 5.1, we get $|\hat{\mathfrak{T}}^h\beta - \mathfrak{T}\beta| \leqslant C_0\bar{p}\gamma^2/2$ for all $|p| \leqslant p_0$. In particular, this estimate holds for $\beta(x,t;\pm\bar{p})$, as for sufficiently large N and M we have $\bar{p} \leqslant p_0$. Furthermore, in view of (5.1), we have $C_1(\varepsilon^2+\bar{p}^2) \leqslant C_1'\bar{p}^2$. As $\bar{p}$ becomes sufficiently small for sufficiently large N and M, we then enjoy $C_1'\bar{p}^2 \leqslant C_0\bar{p}\gamma^2/2$ and therefore $C_0\bar{p}\gamma^2 - C_1(\varepsilon^2+\bar{p}^2) \geqslant C_0\bar{p}\gamma^2/2$. Now, invoking Corollary 4.8 with $p = \pm\bar{p}$, we get $\mathfrak{T}\beta(x,t;-\bar{p}) \leqslant -C_0\bar{p}\gamma^2/2$ and $\mathfrak{T}\beta(x,t;\bar{p}) \geqslant C_0\bar{p}\gamma^2/2$. These bounds immediately imply $\hat{\mathfrak{T}}^h\beta(x_i,t_j;-\bar{p}) \leqslant 0$ and $\hat{\mathfrak{T}}^h\beta(x_i,t_j;\bar{p}) \geqslant 0$; thus we obtained a discrete analogue of estimate (4.29a) in the proof of Theorem 4.9. Using (4.20) and (4.24), we now imitate the remaining part of this proof and conclude that $\beta(x_i,t_j;-\bar{p})$ and $\beta(x_i,t_j;\bar{p})$ are discrete lower and upper solutions. Furthermore, by Lemma 4.6, we have $\beta(x_i,t_j;\pm\bar{p}) = u_{\rm as}(x_i,t_j) + O(\bar{p})$. As, by Proposition 5.2, there exists $\hat{U}_{ij}$ between $\beta(x_i,t_j;-\bar{p})$ and $\beta(x_i,t_j;\bar{p})$, therefore $\hat{U}_{ij} = u_{\rm as}(x_i,t_j) + O(\bar{p})$ and $\hat{U}^I(x,t) = u^I_{\rm as}(x,t) + O(\bar{p})$. Here $u^I_{\rm as}$ is the bilinear interpolant of $u_{\rm as}$, which, by (4.19) combined with (4.7), (4.16), satisfies $u^I_{\rm as}(x,t) = u_{\rm as}(x,t) + O(\bar{p})$; thus $\hat{U}^I(x,t) = u_{\rm as}(x,t) + O(\bar{p})$. Finally, recalling Theorem 4.9 and assumption (5.1), we get $u_{\rm as}(x,t) = u(x,t) + O(\varepsilon^2) = u(x,t) + O(\bar{p})$, which yields the desired estimate for $\hat{U}^I$. □

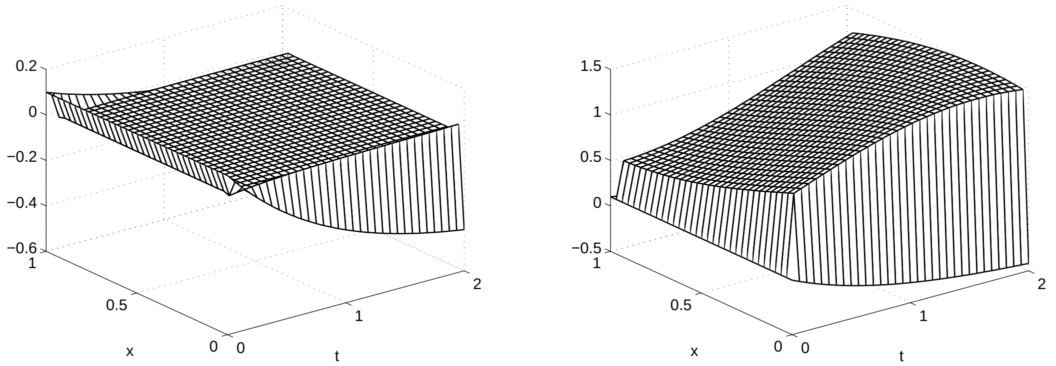

FIG. 3. Uniform mesh in both space and time: conventional method (1.3) fails to produce a correct computed solution (left); stabilized method (2.1) with $\hat{C} = 4$ yields a qualitatively-correct computed solution (right); $\varepsilon = 10^{-4}$, $N = 32$, $M = N^2$, shown time levels $j = 0, N, 2N, \ldots, N^2$.

6. Numerical results

Our model problem is (1.1) in the domain $(x,t) \in [0,1] \times [0,2]$ with

$$f(x,t,u) := (2-u)(u-u_1)u(u-u_2), \quad \text{where } u_1 := 1 - \tfrac{1}{2}\sin(\tfrac{\pi x}{2} - t), \; u_2 := -(x^2 + \tfrac{1}{2}). \tag{6.1}$$

The corresponding reduced problem (1.2) has two stable solutions u_1 and u_2 and two unstable solutions 0 and 2. We use the boundary conditions $g_0(t) = 0.6e^{-t} - 0.5$ and $g_1(t) = 0.2e^{-t} - 0.1$, and the initial condition $\varphi(x) = 0.1$. A calculation shows that the boundary conditions satisfy (A2) for both $u_0 = u_1$ and $u_0 = u_2$. But (A3) is satisfied only for the stable reduced solution $u_0 = u_1$ (in other words, our initial condition is in the domain of attraction of u_1). Therefore, away from $x = 0$, $x = 1$ and $t = 0$, the unique solution $u \approx u_1$; see Figure 2 (left). As we have $f_u(x,t,u_1) \geqslant 1.1$, we use $\gamma = 0.9$ in our calculations.

To solve the discrete nonlinear problems (1.3) and (2.1) at each time level we used Newton's method with the initial guess equal to the computed solution at the previous time level. At least four iterations were performed; then the stopping criterion was applied that both $\max_i |\hat{\mathfrak{I}}^h \hat{U}_{ij}|$ and the difference between two successive iterants should not exceed the tolerance of $5 \cdot 10^{-12}$.

(1) First, we compare the numerical methods (1.3) and (2.1) applied to the test problem (6.1) on a

Table 1. Conventional method (1.3) on the Bakhvalov mesh with $M = N^2$. Computational rates r in $(N^{-1})^r$ (upper part) and maximum nodal errors (lower part).

N	$\varepsilon = 10^{-1}$	$\varepsilon = 10^{-2}$	$\varepsilon = 10^{-3}$	$\varepsilon = 10^{-4}$	$\varepsilon = 10^{-5}$	$\varepsilon = 10^{-6}$	$\varepsilon = 10^{-7}$	$\varepsilon = 10^{-8}$	$\max_\varepsilon$
32	1.94	2.06	2.07	2.07	2.07	2.07	2.07	2.07	2.07
64	2.02	2.01	2.01	2.01	2.01	2.01	2.01	2.01	2.01
128	2.00	2.00	2.00	2.00	2.00	2.00	2.00	2.00	2.00
32	8.02e-3	1.70e-2	1.72e-2	1.72e-2	1.72e-2	1.72e-2	1.72e-2	1.72e-2	1.72e-2
64	2.08e-3	4.09e-3	4.09e-3	4.09e-3	4.09e-3	4.09e-3	4.09e-3	4.09e-3	4.09e-3
128	5.14e-4	1.01e-3	1.01e-3	1.02e-3	1.02e-3	1.02e-3	1.02e-3	1.02e-3	1.02e-3
256	1.28e-4	2.53e-4	2.53e-4	2.53e-4	2.53e-4	2.53e-4	2.53e-4	2.53e-4	2.53e-4

Table 2. Stabilized method (2.1) with $\hat{C} = 4$ on the Bakhvalov mesh with $M = N^2$. Computational rates r in $(N^{-1})^r$ (upper part) and maximum nodal errors (lower part).

N	$\varepsilon = 10^{-1}$	$\varepsilon = 10^{-2}$	$\varepsilon = 10^{-3}$	$\varepsilon = 10^{-4}$	$\varepsilon = 10^{-5}$	$\varepsilon = 10^{-6}$	$\varepsilon = 10^{-7}$	$\varepsilon = 10^{-8}$	$\max_\varepsilon$
32	1.94	2.05	2.06	2.06	2.06	2.06	2.06	2.06	2.06
64	2.02	1.99	1.99	1.99	1.99	1.99	1.99	1.99	1.99
128	2.00	2.05	2.00	2.00	2.00	2.00	2.00	2.00	2.00
32	7.98e-3	1.97e-2	2.00e-2	2.01e-2	2.01e-2	2.01e-2	2.01e-2	2.01e-2	2.01e-2
64	2.08e-3	4.76e-3	4.80e-3	4.81e-3	4.81e-3	4.81e-3	4.81e-3	4.81e-3	4.81e-3
128	5.14e-4	1.19e-3	1.21e-3	1.21e-3	1.21e-3	1.21e-3	1.21e-3	1.21e-3	1.21e-3
256	1.28e-4	2.88e-4	3.01e-4	3.02e-4	3.02e-4	3.02e-4	3.02e-4	3.02e-4	3.02e-4

Table 3. Conventional method (1.3) on the Shishkin mesh with $M = N^2$. Computational rates r in $(N^{-1}\ln(N/4))^r$ (upper part) and maximum nodal errors (lower part).

N	$\varepsilon = 10^{-1}$	$\varepsilon = 10^{-2}$	$\varepsilon = 10^{-3}$	$\varepsilon = 10^{-4}$	$\varepsilon = 10^{-5}$	$\varepsilon = 10^{-6}$	$\varepsilon = 10^{-7}$	$\varepsilon = 10^{-8}$	$\max_\varepsilon$
32	3.34	2.45	2.45	2.45	2.45	2.45	2.45	2.45	2.45
64	2.96	2.04	2.04	2.04	2.04	2.04	2.04	2.04	2.04
128	2.71	2.00	2.01	2.01	2.01	2.01	2.01	2.01	2.00
32	9.37e-3	4.07e-2	4.07e-2	4.07e-2	4.07e-2	4.07e-2	4.07e-2	4.07e-2	4.07e-2
64	2.42e-3	1.51e-2	1.51e-2	1.51e-2	1.51e-2	1.51e-2	1.51e-2	1.51e-2	1.51e-2
128	6.03e-4	5.77e-3	5.77e-3	5.78e-3	5.78e-3	5.78e-3	5.78e-3	5.78e-3	5.78e-3
256	1.51e-4	2.07e-3	2.07e-3	2.07e-3	2.07e-3	2.07e-3	2.07e-3	2.07e-3	2.07e-3

uniform mesh in both space and time; see Figure 3. Similarly to Figure 1, we observe that the conventional method (1.3) fails to produce a correct computed solution (left), while switching to the stabilized method (2.1) with $\hat{C} = 4$ (chosen using Proposition 2.2), we get a qualitatively-correct computed solution (right).

(2) On the layer-adapted meshes of Bakhvalov and Shishkin type, both the numerical methods (1.3) and (2.1) produce qualitatively and quantitatively correct computed solutions. To be more precise, we used the Bakhvalov mesh of §5.1(a) with $C_3 = 2\gamma^{-1}$ and $C_4 = (\gamma^2 T)^{-1}$, and the Shishkin mesh of §5.1(b) with $\ln N$ and $\ln M$ in (5.2) replaced by $\ln(N/4)$ and $\ln(M/2)$ (as Theorem 5.4 also applies to this version of the Shishkin mesh); for both meshes we set $\gamma = 0.9$ and $T = 2$. Tables 1–4 show rates of convergence and maximum nodal errors computed as described in (Kopteva & Stynes, 2004, §4) (for each pair of N and $M = N^2$, a solution on an auxiliary mesh was used with $2N$ and $4M$ mesh intervals in the space and time directions, respectively). Furthermore, the dependence of the error on M is illustrated by Tables 5 and 6, where we fixed $N = 800$ and used the Bakhvalov mesh (similarly, for each M, the rates of convergence and maximum nodal errors were computed using a solution on auxiliary mesh with $N = 800$ and $2M$ mesh intervals in the time direction).

Examining Tables 1–6, we conclude that the errors stabilize as ε approaches 0 and, furthermore, the convergence rates confirm the sharpness of the bounds of Theorem 5.4. Comparing the conventional method (1.3) and the stabilized method (2.1), we observe that although the errors of the stabilized method are slightly larger on the Bakhvalov mesh, on the considered layer-adapted meshes both methods enjoy quite similar ε-uniform convergence.

(3) It should be noted that even on layer-adapted meshes, the conventional scheme (1.3) might have

Table 4. Stabilized method (2.1) with $\hat{C}=4$ on the Shishkin mesh with $M=N^2$. Computational rates r in $(N^{-1}\ln(N/4))^r$ (upper part) and maximum nodal errors (lower part).

N	$\varepsilon=10^{-1}$	$\varepsilon=10^{-2}$	$\varepsilon=10^{-3}$	$\varepsilon=10^{-4}$	$\varepsilon=10^{-5}$	$\varepsilon=10^{-6}$	$\varepsilon=10^{-7}$	$\varepsilon=10^{-8}$	$\max_\varepsilon$
32	3.22	2.55	2.56	2.56	2.56	2.56	2.56	2.56	2.56
64	2.96	2.03	2.03	2.03	2.03	2.03	2.03	2.03	2.03
128	2.71	1.99	1.99	1.99	1.99	1.99	1.99	1.99	1.99
32	8.92e-3	4.13e-2	4.14e-2	4.14e-2	4.14e-2	4.14e-2	4.14e-2	4.14e-2	4.14e-2
64	2.42e-3	1.47e-2	1.47e-2	1.47e-2	1.47e-2	1.47e-2	1.47e-2	1.47e-2	1.47e-2
128	6.03e-4	5.67e-3	5.67e-3	5.67e-3	5.67e-3	5.67e-3	5.67e-3	5.67e-3	5.67e-3
256	1.51e-4	2.06e-3	2.05e-3	2.05e-3	2.05e-3	2.05e-3	2.05e-3	2.05e-3	2.06e-3

multiple discrete solutions, as outlined in Remarks 2.4 and 2.5. E.g., Figure 4 shows that varying the initial guess of Newton's method, which is used at each time level, we get multiple solutions of the same discrete problem (1.3) on the Bakhvalov mesh. Note also that if we switch to the stabilized scheme (2.1) with $\hat{C}=4$, all these initial guesses produce the same correct discrete solution.

(4) Finally, we briefly comment on the *explicit* versions of the conventional method (1.3) and the stabilized method (2.1), obtained by replacing $\delta_t U_{ij}$ with the forward difference $(U_{i,j+1}-U_{ij})/k_{j+1}$. Considering that (1.3) is a particular case of (2.1) with $\hat{\varepsilon}_j=\varepsilon$, our numerical experiments show that one gets stable solutions unless the Stability Condition $\hat{\varepsilon}_j^2/k_j \leqslant 2\varepsilon^2/(h_{i-1}h_i)+\max f_u$ is significantly violated. (Note that under this condition, Proposition 5.2 can be also proved for the explicit method).

Table 5. Conventional method (1.3) on the Bakhvalov mesh with fixed $N=800$. Computational rates r in $(M^{-1})^r$ (upper part) and maximum nodal errors (lower part).

M	$\varepsilon=10^{-1}$	$\varepsilon=10^{-2}$	$\varepsilon=10^{-3}$	$\varepsilon=10^{-4}$	$\varepsilon=10^{-5}$	$\varepsilon=10^{-6}$	$\varepsilon=10^{-7}$	$\varepsilon=10^{-8}$	$\max_\varepsilon$
256	0.92	0.94	0.94	0.94	0.94	0.94	0.94	0.94	0.94
512	0.96	0.97	0.97	0.97	0.97	0.97	0.97	0.97	0.97
1024	0.95	0.98	0.98	0.98	0.98	0.98	0.98	0.98	0.98
256	4.77e-3	5.30e-3	5.30e-3	5.30e-3	5.30e-3	5.30e-3	5.30e-3	5.30e-3	5.30e-3
512	2.52e-3	2.76e-3	2.76e-3	2.76e-3	2.76e-3	2.76e-3	2.76e-3	2.76e-3	2.76e-3
1024	1.29e-3	1.41e-3	1.41e-3	1.41e-3	1.41e-3	1.41e-3	1.41e-3	1.41e-3	1.41e-3
2048	6.69e-4	7.13e-4	7.14e-4	7.14e-4	7.14e-4	7.14e-4	7.14e-4	7.14e-4	7.14e-4

Table 6. Stabilized method (2.1) with $\hat{C}=4$ on the Bakhvalov mesh with fixed $N=800$. Computational rates r in $(M^{-1})^r$ (upper part) and maximum nodal errors (lower part).

M	$\varepsilon=10^{-1}$	$\varepsilon=10^{-2}$	$\varepsilon=10^{-3}$	$\varepsilon=10^{-4}$	$\varepsilon=10^{-5}$	$\varepsilon=10^{-6}$	$\varepsilon=10^{-7}$	$\varepsilon=10^{-8}$	$\max_\varepsilon$
256	0.95	0.99	0.99	0.99	0.99	0.99	0.99	0.99	0.95
512	1.26	0.99	0.99	0.99	0.99	0.99	0.99	0.99	1.14
1024	2.90	1.00	1.00	1.00	1.00	1.00	1.00	1.00	1.00
256	2.32e-2	2.15e-2	2.15e-2	2.15e-2	2.15e-2	2.15e-2	2.15e-2	2.15e-2	2.32e-2
512	1.20e-2	1.08e-2	1.08e-2	1.08e-2	1.08e-2	1.08e-2	1.08e-2	1.08e-2	1.20e-2
1024	5.00e-3	5.44e-3	5.45e-3	5.45e-3	5.45e-3	5.45e-3	5.45e-3	5.45e-3	5.45e-3
2048	6.69e-4	2.73e-3	2.73e-3	2.73e-3	2.73e-3	2.73e-3	2.73e-3	2.73e-3	2.73e-3

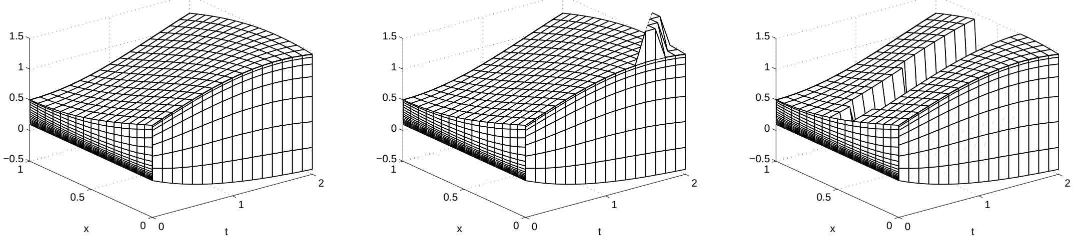

FIG. 4. Multiple discrete solutions of the conventional scheme (1.3) on the Bakhvalov mesh are obtained using Newton's method with various initial guesses equal to: the computed solution at the previous time level (left), 1 (centre), the computed solution at the previous time level multiplied by $1-0.4\sin(\pi x)$ (right); $\varepsilon = 10^{-4}$, $N = 32$, $M = N^2$, shown time levels $j = 0, N, 2N, \ldots, N^2$.

For the test problem (6.1) solved on the uniform mesh using the explicit conventional method, the Stability Condition becomes $M \geqslant 2[2+2.5/(\varepsilon N)^2]N^2$, where we used $\hat{\varepsilon}_j = \varepsilon$, $k_j = 2M^{-1}$, $h_i = N^{-1}$ and $\max f_u \approx 2.5$. If the explicit stabilized method is used, the Stability Condition becomes much less stringent as now it suffices to satisfy $\hat{C} \geqslant 2(\varepsilon N) + 2.5$ if the stability condition for the conventional method is violated.

However, the Stability Condition becomes very restrictive wherever the mesh is fine in space and standard in time, e.g., for $j > M/2$ on the layer-adapted meshes of §5.1. In this case f_u is negligible compared to ε^2/h_i^2, and the Stability Condition is effectively equivalent to $k_j \leqslant \frac{1}{2}h_i^2$ for the explicit conventional method and $k_j \leqslant \frac{1}{2}h_i^2(\hat{\varepsilon}_j^2/\varepsilon^2)$ for the explicit stabilized method. Consider the explicit conventional method applied to the test problem (6.1) on the Bakhvalov mesh (the results on the Shishkin mesh are similar). Our numerical experiments show that for $\varepsilon = 10^{-2}$, $N = 32$, $M = 400N^2$, starting from $j = M/2+1$, the computed solution exhibits oscillations which rapidly grow in time, i.e. the method is unstable (note that on this mesh $\max\{k_j/h_i^2\} \approx 1.08$). Now, switching to $M = 800N^2$ produces a stable method (with $\max\{k_j/h_i^2\} \approx 0.55$). Next, we set $\varepsilon = 2\cdot 10^{-2}$, $N = 32$, and observe that $M = 100N^2$ yields an unstable method (with $\max\{k_j/h_i^2\} \approx 1.12$), while $M = 200N^2$ yields a stable method (with $\max\{k_j/h_i^2\} \approx 0.56$).

For the explicit version of the stabilized method, the Stability Condition $k_j \leqslant \frac{1}{2}h_i^2(\hat{\varepsilon}_j^2/\varepsilon^2)$ seems less severe as it suffices to satisfy either the stability condition for the explicit method, or $\hat{C}^{-1} \leqslant \frac{1}{2}h_i^2/\varepsilon^2$. However on the considered layer adapted meshes, we have $\min\{h_i\} = C\varepsilon N^{-1}\ln^m N$, so the latter inequality cannot be satisfied for sufficiently large N. In agreement with this heuristic argument, our numerical experiments show that the same restrictive stability condition applies to the explicit version of the stabilized method.

In summary, our numerical experiments on both uniform and layer-adapted meshes suggest that the stability condition for the explicit stabilized method is $\hat{\varepsilon}_j^2/k_j \leqslant 2\varepsilon^2/h_i^2 + \max f_u$, and confirm that this condition is very restrictive on certain layer-adapted meshes.

7. Conclusions

We have shown that the conventional implicit method (1.3) might produce incorrect and unstable computed solutions on uniform meshes; see Figures 1 and 3. Therefore we propose a stabilized method (2.1), in which the added stabilization is controlled by a constant parameter $\hat{C} \geqslant 0$. For this method, Proposition 2.2 prescribes a choice of $\hat{C}$ that ensures at most one discrete solution (similarly to the original problem). Furthermore, our numerical results suggest that under this choice of $\hat{C}$, switching to the stabilized method cures the instability and yields qualitatively-correct computed solutions on any mesh.

We theoretically investigated these two methods on layer-adapted meshes of Bakhvalov and Shishkin types and established their second-order convergence in space and first-order convergence in time (with, in the case of the Shishkin mesh, a logarithmic factor) in the maximum norm, for $\varepsilon \leqslant C(N^{-1}+M^{-1/2})$; see Theorem 5.4.

Although both considered methods yield accurate computed solutions on layer-adapted meshes, we note that the conventional method (1.3) is unstable on certain meshes, which might be unacceptable, e.g., if a layer-adapted mesh is constructed adaptively, starting from an unsophisticated initial mesh. Therefore we advocate the stabilized method (2.1) over the conventional method (1.3).

REFERENCES

BAKHVALOV, N.S. (1969) Towards optimization of methods for solving boundary value problems in the presence of a boundary layer, *Zh. Vychisl. Mat. i Mat. Fiz.,* **9**, 841–859 (in Russian).

FIFE, P.C. (1973) Semilinear elliptic boundary value problems with small parameters, *Arch. Rational Mech. Anal.,* **52**, 205–232.

FIFE, P.C. & GILL, G.S. (1991) Phase-transition mechanisms for the phase-field model under internal heating, *Phys. Rev. A (3),* **43**, 843–851.

KOPTEVA, N. (2007) Maximum norm error analysis of a 2d singularly perturbed semilinear reaction-diffusion problem, *Math. Comp.,* **76**, 631–646.

KOPTEVA, N. & STYNES, M. (2004) Numerical analysis of a singularly perturbed nonlinear reaction-diffusion problem with multiple solutions, *Appl. Numer. Math.,* **51**, 273-288.

LORENZ, J. (1981) Nonlinear singular perturbation problems and the Enquist-Osher scheme, *Mathematical Institute, Catholic Univerity of Nijmegen,* Report 8115 (unpublished).

MILLER, J.J.H., O'RIORDAN, E. & SHISHKIN, G.I. (1996) *Fitted Numerical Methods for Singular Perturbation Problems*. Singapore: World Scientific.

NEFEDOV, N.N. (1995) The method of differential inequalities for some classes of nonlinear singularly perturbed problems with internal layers, *(Russian) Differ. Uravn.,* **31**, 1142–1149; translation in *Differ. Equ.,* 1077–1085.

PAO, C.V. (1985) Monotone iterative methods for finite difference system of reaction-diffusion equations, *Numer. Math.,* **46**, 571–586.

PAO, C.V. (1992) *Nonlinear parabolic and elliptic equations*. New York: Plenum Press.

PROTTER, M.H. & WEINBERGER, H.F. (1999) *Maximum principles in differential equations*. New York: Springer-Verlag.

ROOS, H.-G., STYNES, M. & TOBISKA, L. (2008) *Robust Numerical Methods for Singularly Perturbed Differential Equations*. Berlin: Springer-Verlag.

SHISHKIN, G.I. (1992) *Grid approximation of singularly perturbed elliptic and parabolic equations*. Ekaterinburg: Ur. O. RAN (in Russian).

SOANE, A.M., GOBBERT, M.K. & SEIDMAN, T.I. (2005) Numerical exploration of a system of reaction-diffusion equations with internal and transient layers, *Nonlinear Anal. Real World Appl.,* **6**, 914–934.

SUN, G. & STYNES, M. (1996) A uniformly convergent method for a singularly perturbed semilinear reaction-diffusion problem with multiple solutions, *Math. Comp.,* **65**, 1085–1109.

VASIL'EVA, A.B., BUTUZOV, V.F. & KALACHEV, L.V. (1995) *The boundary function method for singular perturbation problems*. Philadelphia: SIAM.

WINFREE, A.T. & JAHNKE, W. (1989) Three-dimensional scroll ring dynamics in the Belousov-Zhabotinsky reagent and in the two-variable Oregonator model, *J. Phys. Chem.,* **93**, 2823–2832.